Passive Bilateral Feedforward Control of Linear Dynamically Similar Teleoperated Manipulators

Dongjun Lee, *Student Member, IEEE,* and Perry Y. Li, *Member, IEEE*

***Abstract*—This paper presents a passive bilateral feedforward control scheme for linear dynamically similar (LDS) teleoperated manipulators with kinematic scaling and power scaling. The proposed control law renders the teleoperator as a passive rigid mechanical tool with programmable apparent inertia to the human operator and the work environment by utilizing bilateral force feedforward and kinematic feedback control. The passivity of the closed-loop system is robust to force measurement inaccuracies and model uncertainty. Thus, interaction stability of the teleoperator with any passive environment is guaranteed. Coordination error and the overall motion aspects of teleoperation are controlled individually. The proposed control law is also applicable to general nonlinear robotic teleoperators if sufficiently high kinematic feedback gains are used. The proposed control schemes have been validated experimentally for both LDS and non-LDS systems.**

***Index Terms*—Apparent inertia, decomposition, dynamic similarity, feedforward, kinematic scaling, passivity, power scaling.**

I. Introduction

A teleoperated manipulator is a two-port system which interacts mechanically with the human operator and the work environment simultaneously. An *a priori* requirement is that it can interact and physically couple with a broad class of environments without becoming unstable. A teleoperator that is stable on its own may not be stable when interacting with a stable environment or human operator, as the interconnection between two individually stable systems does not necessarily result in a stable system. Arguably, coupling stability is even more important for teleoperator with force or power amplification/attenuation capabilities, when delicate environment is involved, or when safety is a first priority (e.g., in robotic surgery). It is well known that the coupling between a passive system and another strictly passive system with compatible supply rates is necessarily stable (see, e.g., [1]). Moreover, most physical objects are strictly passive, and the mechanical impedances of human musculoskeletal systems have been shown to be indistinguishable from that of a passive object [2]. Therefore, many authors have used passivity to define safety for systems that interact with humans and physical environments [3]–[5].

The emphasis in many previous works on the control of teleoperators (such as [6], [7]) is to transfer precisely the mechanical impedance that the slave robot experiences to the human operator. Such *ideal transparency* is only possible when the teleoperator does not present any intervening or apparent inertia to the human operator or the work environment [7]. Controls that attain ideal transparency generally require the knowledge of human and environment impedances, either as a predetermined model [8] or by the use of an online impedance estimator [6]. The range and the time varying nature of the human and environment impedances [2] make it a challenge either to model the environments by a single tractable mathematical model or to design an estimator that estimates the impedances sufficiently quickly. Because of this, a control scheme was proposed in [9] (and later adopted in [10] and [11]) which does not require knowledge of the impedances of the human operator and the work environment. Using both force and state measurements, this control scheme achieves transparency in the low-frequency range. However, as is pointed out in [12], passivity of the system cannot be guaranteed when force measurement is inaccurate. Even 5% error in force measurements can destabilize the system.

Our control philosophy for bilateral teleoperators [13] is not primarily to achieve ideal transparency, but to present the teleoperator as a **common passive rigid mechanical tool**, to both the human operator and the work environment. As such, the teleoperator should appear to the human as a mechanical extension of his/her body, much like a cane, a tennis racket, or a passive prosthesis, which humans can learn to use dextrously, and which often provide humans with an extended physiological proprioception (EPP) [14], [15]. Unlike an ordinary passive mechanical tool, such a teleoperator can also provide the desired kinematic and power scalings, thus enabling the operator to effectively change size, strength, and sensitivity. In addition, the apparent natural dynamics of the "locked system" (i.e., the rigidly coordinated system that results after the master and slave manipulators have been rigidly coordinated according to the desired kinematic scaling) can be designed to facilitate the task at hand. For example, large apparent inertias can be programmed for hammering tasks and small inertias for probing tasks; suitable natural dynamics can be programmed for path guidance or obstacle avoidance, etc. By enforcing a suitable passivity property that takes into account power scaling in the control design, coupling stability between the teleoperator and the human and

Manuscript received March 19, 2002; revised October 25, 2002. This paper was recommended for publication by Associate Editor Y. Liu and Editor I. Walker upon evaluation of the reviewers' comments. This work was supported by the National Science Foundation under Grant CMS-9870013. This paper was presented in part at ACC, Philadelphia, PA, 1998; IMECE, Orlando, FL, 2000; and ACC, Arlington, VA, 2001.

The authors are with the Department of Mechanical Engineering, University of Minnesota, Minneapolis, MN 55455 USA (e-mail: djlee@me.umn.edu; pli@me.umn.edu).

Digital Object Identifier 10.1109/TRA.2003.810576

the work environments becomes less of an issue. For an environment to destabilize a passive teleoperator, it has to be active (nonpassive) and typically has to supply an infinite amount of energy. Thus, teleoperators that mimic passive rigid mechanical tools would be potentially safer.

Working independently, the authors in [16] also embrace a similar control philosophy. Their concept of *task-oriented virtual tool* is essentially the same as our common passive mechanical tool. The key difference lies in the controller structures. The control law in [16] uses full information (including human and environment force) feedback to exactly cancel the open-loop dynamics of the teleoperator first, and then installs the desired passive dynamics of the virtual tool. Although the control law is easily understandable, passivity, which is related to safety, may be compromised when the open-loop dynamics are not perfectly canceled out, such as in the presence of model uncertainty or inaccurate force measurements. Our approach in this and previous papers [13], [17], [18], is to enforce passivity in a robust manner by an appropriate controller structure. Our intention is to allow performance to degrade in the presence of model uncertainties or force measurement inaccuracies, while ensuring that passivity is still preserved.

Following [13], we design controllers based on linear dynamically similar (LDS) teleoperators. A pair of n-degree of freedom (DOF) LDS manipulators can be decomposed, both *dynamically* and *energetically*, into two n-DOF mechanical systems [13]. The decomposed systems, which we refer to as *shape* and *locked* systems, represent the coordination and the gross motion, respectively. Thus, passivity of the overall system and the two aspects of teleoperation (rigid coordination and installing desired rigid mechanical tool dynamics) can be achieved by controlling the *shape* and *locked* systems separately, and by ensuring that they are individually passive. This formulation allows the control law to be designed and analyzed completely in the time domain, so that the main ideas may be extended to general nonlinear manipulators. This is unlike other previous works on teleoperators or haptic systems, most of which also deal with linear models [3], [6]–[9], [11], [19]–[21], but use frequency domain formulations that are not easy to extend to the nonlinear setting.

The *shape* system concept enables coordination to be explicitly specified as a control objective, similiar to other coordination/synchronization control approaches prevalent in machining and multirobot coordination (e.g., [22], [23] and references therein), with the extra requirement that the control must preserve passivity. The passive shape system (coordination) control law in [13] was designed based on the passive velocity field control (PVFC) technique [24]–[27]. It assumes only kinematic feedback, so coordination degrades in the presence of mismatched operator and environment forcing. Moreover, the apparent inertia of the teleoperator is not programmable. To remedy these problems, we propose a passive feedforward control law that enables the rigid coordination in the presence of arbitrary human-environment forcing, and also allows the desired locked system dynamics to have programmable apparent inertia. By measuring the forces at the master and the slave systems, a feedforward action compensates for any mismatched operator/environment force to achieve perfect rigidity and programmable apparent inertia. The feedforward action is implemented in a robustly passive manner by the use of fictitious energy storages and the skew-symmetric or negative semidefinite feedback structure. The kinematic feedback portion of the controller has also been redesigned from [13] to achieve a better convergence rate.

Although the proposed control law is derived for LDS systems, it is also applicable to general multi-DOF nonlinear teleoperators. Using sufficiently high kinematic feedback gains, coordination error can be arbitrarily reduced. This enables the teleoperator dynamics to be close to the desired target dynamics. Recently, the ideas set forth in this paper were extended in [28] and [29] to fully address the nonlinear teleoperator control problem.

The rest of the paper is organized as follows. In Section II, the control problem is formulated. In Section III, the decomposition of LDS teleoperated manipulators into dynamically and energetically decoupled *shape* and *locked* systems is presented. Control for the shape system is discussed in Section IV, whereas control for the locked system is discussed in Section V. Application of the proposed control to nonlinear robotic teleoperators is analyzed in Section VII. Experimental results are presented in Section VIII. Section IX contains some concluding remarks.

II. Problem Formulation

A. Plant

Consider a teleoperated manipulator system consisting of two linear n-DOF manipulators with dynamics given by

$$\mathbf{M}_1\ddot{\mathbf{q}}_1 = \mathbf{T}_1 + \mathbf{F}_1, \qquad \mathbf{M}_2\ddot{\mathbf{q}}_2 = \mathbf{T}_2 + \mathbf{F}_2 \tag{1}$$

where $\mathbf{T}_1, \mathbf{T}_2 \in \Re^n$ are the control forces, $\mathbf{F}_1, \mathbf{F}_2 \in \Re^n$ are the environment forces that the master and slave systems encounter, and $\mathbf{M}_1$ and $\mathbf{M}_2 \in \Re^{n\times n}$ are the inertia matrices for the manipulators.

Let $\alpha \in \Re^{n\times n}$ be the desired bijective linear *kinematic scaling*. Ideally, we would like

$$\alpha_1\mathbf{q}_1(t) = \mathbf{q}_2(t) \tag{2}$$

so that the system achieves perfect coordination (locking).

We assume that the slave and master manipulators are **dynamically similar with respect to** α [30] in the sense that there exists a scalar $\zeta > 0$, s.t.

$$\zeta\mathbf{M}_1 = \alpha^T\mathbf{M}_2\alpha. \tag{3}$$

The assumption that the teleoperated manipulator is LDS is an idealization that the master and slave robots are similarly constructed when the relative dimensions, determined by the kinematic scaling α, are taken into account. Any linear 1-DOF mechanical system automatically satisfies this property.

B. Energetic Passivity With Power Scaling

To ensure that both the human and the work environment can interact with the teleoperated manipulator in stable fashion, we require that the teleoperator be energetically passive with a

power scaling ρ. Let us define the supply rate to be the scaled power input given by

$$s_\rho(\dot{\mathbf{q}}_1, \dot{\mathbf{q}}_2, \mathbf{F}_1, \mathbf{F}_2) = \rho \mathbf{F}_1^T \dot{\mathbf{q}}_1 + \mathbf{F}_2^T \dot{\mathbf{q}}_2 \tag{4}$$

which is the sum of the power exerted by the force $\mathbf{F}_2$ and ρ times of the power exerted by the force $\mathbf{F}_1$. We require that the closed-loop controlled teleoperated system satisfy

$$\int_0^t s_\rho(\dot{\mathbf{q}}_1(\tau), \dot{\mathbf{q}}_2(\tau), \mathbf{F}_1(\tau), \mathbf{F}_2(\tau))\, d\tau \geq -c^2, \quad \forall t \geq 0 \tag{5}$$

for some $c \in \Re$, which would depend on the initial condition at $t = 0$. We call such systems energetically passive with power scaling ρ to emphasize the fact that the supply rate in (4) is associated with physical power. Equation (5) expresses the condition that the amount of scaled energy that can be extracted by the human and work environment is limited by the initial stored energy c^2.

The supply rate defined in (4) which incorporates power scaling inspires the following definition of scaled kinetic energy for the teleoperated manipulator system:

$$\kappa_\rho(\dot{\mathbf{q}}_1, \dot{\mathbf{q}}_2) = \frac{\rho}{2} \dot{\mathbf{q}}_1^T \mathbf{M}_1 \dot{\mathbf{q}}_1 + \frac{1}{2} \dot{\mathbf{q}}_2^T \mathbf{M}_2 \dot{\mathbf{q}}_2 \geq 0. \tag{6}$$

Our control objective is to design the control actions $\mathbf{T}_1$ and $\mathbf{T}_2$ so that: 1) the teleoperator system in (1) is rigidly coordinated according to (2); 2) the overall motion of the teleoperator mimics some desired dynamics with adjustable apparent inertia (to be given later); and 3) the closed-loop system is energetically passive with power scaling ρ as in (4) and (5).

III. Decomposition Into Shape and Locked Systems

In this section, we decompose the dynamics of the teleoperator system into two systems according to two aspects of the teleoperation: gross motion (*locked system*) and coordination (*shape system*). It will be shown that for LDS teleoperated manipulators, the two resulting systems can be individually controlled, and as long as the individual controller is designed such that each closed-loop system is energetically passive, the combined teleoperator system is also energetically passive.

Let $\mathbf{E} = (\zeta/(\rho+\zeta))[\alpha \mathbf{q}_1 - \mathbf{q}_2]$ be the coordination error, and consider the constant coordinate transformation of the velocity space (i.e., tangent bundle)

$$\begin{pmatrix} \mathbf{V}_L \\ \dot{\mathbf{E}} \end{pmatrix} = \underbrace{\frac{\zeta}{\rho+\zeta} \begin{bmatrix} \frac{\rho}{\zeta}\alpha & \mathbf{I} \\ \alpha & -\mathbf{I} \end{bmatrix}}_{\mathbf{S}} \begin{pmatrix} \dot{\mathbf{q}}_1 \\ \dot{\mathbf{q}}_2 \end{pmatrix}. \tag{7}$$

Similarly, consider the compatible transformation of the controls and forces

$$\begin{pmatrix} \mathbf{T}_L \\ \mathbf{T}_E \end{pmatrix} = \mathbf{S}^{-T} \begin{pmatrix} \rho \mathbf{T}_1 \\ \mathbf{T}_2 \end{pmatrix}, \quad \begin{pmatrix} \mathbf{F}_L \\ \mathbf{F}_E \end{pmatrix} = \mathbf{S}^{-T} \begin{pmatrix} \rho \mathbf{F}_1 \\ \mathbf{F}_2 \end{pmatrix}. \tag{8}$$

Here, $\mathbf{T}_L$ and $\mathbf{T}_E$ are the controls and $\mathbf{F}_L$ and $\mathbf{F}_E$ are the human and work environment forcing on the system in the transformed coordinates. Under transformations (7) and (8), the dynamics of the LDS teleoperator system (1) block diagonalizes into

$$\mathbf{M}_L \dot{\mathbf{V}}_L = \mathbf{T}_L + \mathbf{F}_L \tag{9}$$

$$\mathbf{M}_E \ddot{\mathbf{E}} = \mathbf{T}_E + \mathbf{F}_E \tag{10}$$

where

$$\mathbf{M}_L = \mathbf{M}_2 + \rho \alpha^{-T} \mathbf{M}_1 \alpha^{-1},$$
$$\mathbf{M}_E = \frac{\rho(\zeta+\rho)}{\zeta^2} \mathbf{M}_2. \tag{11}$$

The n-DOF mechanical system in (9) is referred to as the *locked* system, since it represents the gross motion of the two manipulators when they are perfectly coordinated (locked). The other n-DOF mechanical system in (10) will be referred to as the *shape* system, since it determines the coordination aspect of the two manipulators. $\mathbf{M}_L$ and $\mathbf{M}_E$ are referred to as the locked and shape system inertias, respectively. Here, $(\mathbf{T}_L, \mathbf{F}_L)$ are, respectively, the controls and the human and environment forcing on the locked system, and $(\mathbf{T}_E, \mathbf{F}_E)$ are those on the shape system. Fig. 1 illustrates this transformation when $\rho = \alpha = 1$ for a pair of 1-DOF teleoperated robots.

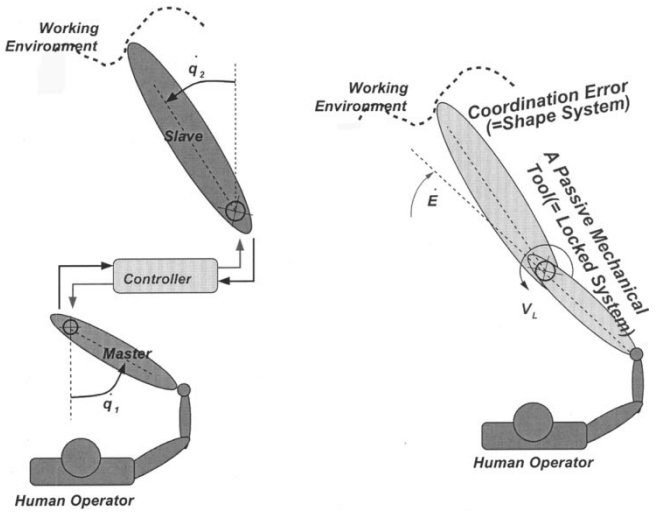

Fig. 1. For the teleoperator having two 1-DOF planar manipulators and with $\alpha = 1$ and $\rho = 1$, the locked system represents the passive rigid tool which is obtained by connecting the two 1-DOF planar manipulators rigidly (locked), whereas the shape system represents the coordination aspects of teleoperation (i.e., rigidity of the tool). Notice that if $\zeta = 1$, then $\mathbf{V}_L = (1/2)(\dot{\mathbf{q}}_1 + \dot{\mathbf{q}}_2)$ and $\dot{\mathbf{E}} = (1/2)(\dot{\mathbf{q}}_1 - \dot{\mathbf{q}}_2)$.

Remarkably, with the coordinate transformation (7), the scaled kinetic energy (6) is the sum of the kinetic energies of the *shape* and the *locked* systems

$$\kappa_\rho(\dot{\mathbf{q}}_1, \dot{\mathbf{q}}_2) = \frac{1}{2} \mathbf{V}_L^T \mathbf{M}_L \mathbf{V}_L + \frac{1}{2} \dot{\mathbf{E}}^T \mathbf{M}_E \dot{\mathbf{E}}. \tag{12}$$

Moreover, because of (7) and (8), the supply rate in (4) is the sum of the usual individual supply rates of the *locked* and *shape* systems

$$s_\rho(\dot{\mathbf{q}}_1, \dot{\mathbf{q}}_2, \mathbf{F}_1, \mathbf{F}_2) = \mathbf{F}_L^T \mathbf{V}_L + \mathbf{F}_E^T \dot{\mathbf{E}}. \tag{13}$$

The following proposition is a direct consequence of the fact that the locked and the shape systems are a decomposition of

both the dynamics (9) and (10) as well as the kinetic enegy (12) of the LDS teleoperated manipulators.

Proposition 1: Consider the LDS teleoperated manipulator in (1). If its *locked* and *shape* systems in (9) and (10) are individually controlled using $\mathbf{T}_L$ and $\mathbf{T}_E$, respectively, such that each system is individually passive, i.e., $\exists c_L, c_E$ s.t. $\forall \mathbf{F}_L, \mathbf{F}_E$, and $\forall t \geq 0$

$$\int_0^t \mathbf{F}_L^T \mathbf{V}_L d\tau \geq -c_L^2, \quad \int_0^t \mathbf{F}_E^T \dot{\mathbf{E}} d\tau \geq -c_E^2 \tag{14}$$

then, the teleoperator system (1) is passive with respect to the supply rate $s_\rho(\dot{\mathbf{q}}_1, \dot{\mathbf{q}}_2, \mathbf{F}_1, \mathbf{F}_2)$ in (4) (i.e., (5) is satisfied).

Proof: Integrating (13) and making use of (14), we have

$$\int_0^t s_\rho\left(\dot{\mathbf{q}}_1(\tau), \dot{\mathbf{q}}_2(\tau), \mathbf{F}_1(\tau), \mathbf{F}_2(\tau)\right) d\tau = \int_0^t \mathbf{F}_L^T \mathbf{V}_L d\tau + \int_0^t \mathbf{F}_E^T \dot{E} d\tau \geq -c_L^2 - c_E^2 = -c^2.$$

■

Thus, it suffices to control the *locked* and *shape* system *independently* so that they are individually passive, and that their individual objectives are satisfied. The control objective for the *shape* system is grid coordination, i.e., to regulate ($\mathbf{E}$, $\dot{\mathbf{E}}$) at ($\mathbf{0}$, $\mathbf{0}$); while the objective for the *locked* system control is to realize some prescribed target dynamics which will be given in Section V.

IV. Shape System Control

A. Shape System Controller Structure

From (10), the shape system dynamics are given by

$$\mathbf{M}_E \ddot{\mathbf{E}} = \mathbf{T}_E + \mathbf{F}_E \tag{15}$$

where $\mathbf{T}_E$ and $\mathbf{F}_E$ are the transformed control torque and mismatched excitation by the human operator and the work environment. We wish to design a control law for $\mathbf{T}_E$ so that the shape system dynamics is passive in the sense of (14) and the coordination error ($\mathbf{E}$, $\dot{\mathbf{E}}$) converges to ($\mathbf{0}$, $\mathbf{0}$).

Since we assume that $\mathbf{F}_1$ and $\mathbf{F}_2$ (and hence, $\mathbf{F}_E$) are available from the force sensors, the following control law, that has a feedback and a feedforward component, would achieve coordination:

$$\mathbf{T}_E = -\mathbf{K}\mathbf{E} - \mathbf{B}\dot{\mathbf{E}} - \mathbf{F}_E \tag{16}$$

where $\mathbf{K}, \mathbf{B} \in \Re^{n \times n}$ are symmetric and strictly positive definite.

Unfortunately, direct implementation of (16) does not preserve passivity in the sense of (14) robustly in the presence of inaccurate $\mathbf{F}_E$ measurements. We propose a control structure that uses a negative semidefinite feedback and two fictitious energy storage elements. As will be discussed in Section VI, the control structure also preserves passivity in the presence of model uncertainty.

One energy storage is the potential energy stored in a fictitious spring $\mathbf{K} \in \Re^{n \times n}$, and the other is associated with the kinetic energy of a fictitious flywheel with dynamics

$${}^E M_f {}^E \ddot{x}_f = {}^E T_f \tag{17}$$

where ${}^E M_f > 0 \in \Re$ and ${}^E x_f \in \Re$ are the constant inertia and the configuration of the flywheel, respectively, and ${}^E T_f$ is the torque input (to be defined) to the flywheel. Energy stored in the flywheel will be used to generate the feedforward cancellation in (16) without violating passivity. The fictitious elements are implemented in the controller.

Define the total energy of the shape system augmented by the fictitious energy storages by

$$\kappa_E(t) := \frac{1}{2}\dot{\mathbf{E}}^T \mathbf{M}_E \dot{\mathbf{E}} + \frac{1}{2}\mathbf{E}^T \mathbf{K} \mathbf{E} + \frac{1}{2} {}^E\mathbf{M}_f {}^E\dot{x}_f{}^2. \tag{18}$$

If $\mathbf{T}_E$ and ${}^E T_f$ are defined to have the structure

$$\begin{pmatrix} \mathbf{K}\dot{\mathbf{E}} \\ \mathbf{T}_E \\ {}^E\mathbf{T}_f \end{pmatrix} = \mathbf{\Omega}_E(t) \begin{pmatrix} \mathbf{E} \\ \dot{\mathbf{E}} \\ {}^E\dot{x}_f \end{pmatrix} \tag{19}$$

where $\mathbf{\Omega}_E(t) \in \Re^{(2n+1)\times(2n+1)}$ is negative semidefinite, then differentiating (18) gives

$$\frac{d}{dt}\kappa_E(t) = \begin{pmatrix} \mathbf{E}^T & \dot{\mathbf{E}}^T & {}^E\dot{x}_f \end{pmatrix} \mathbf{\Omega}_E(t) \begin{pmatrix} \mathbf{E} \\ \dot{\mathbf{E}} \\ {}^E\dot{x}_f \end{pmatrix} + \mathbf{F}_E^T \dot{\mathbf{E}} \leq \mathbf{F}_E^T \dot{\mathbf{E}}.$$

Hence

$$-\kappa_E(0) \leq \kappa_E(t) - \kappa_E(0) \leq \int_0^t \mathbf{F}_E^T(\tau)\dot{\mathbf{E}}(\tau) d\tau.$$

Therefore, the control structure (19) guarantees passivity of the shape system in the sense of (14) regardless of the accuracy of the force measurements.

The negative semidefinite matrix $\mathbf{\Omega}_E(t)$ is designed to be

$$\mathbf{\Omega}_E(t) = \underbrace{\begin{pmatrix} 0 & \mathbf{K} & 0 \\ -\mathbf{K} & -\mathbf{S}_{fb}(t) & -\mathbf{U}_{fb}(t) \\ 0 & \mathbf{U}_{fb}^T(t) & 0 \end{pmatrix}}_{\text{kinematic feedback}} + \underbrace{\begin{pmatrix} 0 & 0 & 0 \\ 0 & -\mathbf{S}_{ff}(t) & -\mathbf{U}_{ff}(t) \\ 0 & \mathbf{U}_{ff}^T(t) & 0 \end{pmatrix}}_{\text{feedforward}} \tag{20}$$

where $\mathbf{S}_{fb}(t)$ is a positive semidefinite matrix that provides the damping effect with $\mathbf{U}_{fb}(t)$, and $\mathbf{S}_{ff}(t) = -\mathbf{S}_{ff}^T(t)$ and $\mathbf{U}_{ff}(t)$ are responsible for the feedforward cancellation of $\mathbf{F}_E$ in (16). The controller structure (19), (20) ensures that energy is not generated by the controller. The flywheel serves as an energy reservoir to generate the feedforward cancellation and is replenished by the damping term. If (16) is implemented directly, the damping term dissipates the energy and the energy required for the feedforward action must be generated by the controller. Thus, passivity of the closed-loop system will not generally be preserved.

The elements in $\mathbf{\Omega}_E(t)$ are designed so that 1) they are always well-behaved (bounded), and 2) that $\mathbf{T}_E$ in (19) approximates the ideal control (16), as follows.

$\mathbf{S}_{fb}(t)$ and $\mathbf{U}_{fb}(t)$ are defined s.t.

$$\mathbf{S}_{fb}(t)\dot{\mathbf{E}} + \mathbf{U}_{fb}(t)^E\dot{x}_f = \mathbf{B}\dot{\mathbf{E}}.$$

Hence, a constant damping effect with $\mathbf{B} \in \Re^{n\times n}$ is achieved. One possibility is to define

$$\mathbf{U}_{fb}(t) = g(t)\mathbf{B}\dot{\mathbf{E}}(t), \quad \mathbf{S}_{fb}(t) = \big(1 - g(t)^E\dot{x}_f(t)\big)\mathbf{B} \tag{21}$$

where

$$g(t) = \begin{cases} \frac{1}{{}^E\dot{x}_f(t)} & \left|{}^E\dot{x}_f(t)\right| > f_0 \\ \frac{1}{f_0}\text{sign}\left({}^E\dot{x}_f(t)\right) & 0 \neq \left|{}^E\dot{x}_f(t)\right| \leq f_0 \\ \frac{1}{f_0} & \left|{}^E\dot{x}_f(t)\right| = 0 \end{cases} \tag{22}$$

and $f_0 > 0$ is a threshold on the flywheel speed ${}^E\dot{x}_f$ to ensure that $\mathbf{U}_{fb}(t)$ and $\mathbf{S}_{fb}(t)$ are well behaved.

Unlike regular damping, the damping effect in the controller is at least partially implemented using the flywheel. The extent of this depends on $g(t)$, and hence, the flywheel speed ${}^E\dot{x}_f(t)$. Instead of a damper simply dissipating the energy, the energy developed in the damper is recaptured in the flywheel. The stored flywheel energy is then used for the feedforward cancellation of $\mathbf{F}_E$ without violating passivity.

The matrices $\mathbf{S}_{ff}(t)$ and $\mathbf{U}_{ff}(t)$ are responsible for the feedforward cancellation. They are designed so that

$$\begin{bmatrix} -\mathbf{S}_{ff}(t) & -\mathbf{U}_{ff}(t) \\ \mathbf{U}_{ff}^T(t) & 0 \end{bmatrix} \begin{pmatrix} \dot{E} \\ {}_{E\dot{x}f} \end{pmatrix} = p(t) \begin{pmatrix} -\mathbf{F}_E \\ \frac{1}{{}^E\dot{x}_f}\mathbf{F}_E^T\dot{\mathbf{E}} \end{pmatrix} \tag{23}$$

where $\mathbf{S}_{ff}(t) \in \Re^{n\times n}$ is a skew-symmetric matrix to ensure that the feedforward action preserves passivity, and $p(t) \in \{0, 1\}$ is a binary switching function to turn on/off the feedforward action according to the energy level of the flywheel, and is defined as

$$p(t) = \begin{cases} 1, & \text{if}({}^E\dot{x}_f, \mathbf{E}, \dot{\mathbf{E}}) \in \mathcal{C} \text{ at time } t \\ 0, & \text{otherwise} \end{cases} \tag{24}$$

where $\mathcal{C} \subset \{({}^E\dot{x}_f, \mathbf{E}, \dot{\mathbf{E}}) \in \Re^{2n+1}\}$ is a nearly invariant region (Fig. 2) to be defined later. Roughly speaking, $\mathcal{C}$ is defined to ensure that once $({}^E\dot{x}_f, \mathbf{E}, \dot{\mathbf{E}})$ enters $\mathcal{C}$, the feedforward action will remain turned on at all future times without depleting the flywheel energy.

A possible set of definitions for $\mathbf{S}_{ff}(t)$ and $\mathbf{U}_{ff}(t)$ is

$$\mathbf{S}_{ff}(t) = \mathbf{0}, \quad \mathbf{U}_{ff}(t) = \begin{cases} \frac{1}{{}^E\dot{x}_f}\mathbf{F}_E, & \text{if } p(t) = 1 \\ \mathbf{0}, & \text{otherwise} \end{cases}$$

The purpose of the thresholding function $g(t)$ in (22) and the switching function $p(t)$ in (24) are to ensure that the matrix $\mathbf{\Omega}_E(t)$ in (19) remains bounded, when the flywheel energy is low. Therefore, we should have $\mathcal{C} \subset \{({}^E\dot{x}_f, \mathbf{E}, \dot{\mathbf{E}}) || {}^E\dot{x}_f| \geq f_0\}$, where f_0 is the threshold flywheel speed in (22). Typically $({}^E\dot{x}_f, \mathbf{E}, \dot{\mathbf{E}})$ would belong to $\mathcal{C}$ if $|{}^E\dot{x}_f|$ is sufficiently large, and/or the error $(\mathbf{E}, \dot{\mathbf{E}})$ are sufficiently small.

When force sensor measurement is accurate, the dynamics of the shape system (10) under the control law (19)–(23) become

$$\mathbf{M}_E\ddot{\mathbf{E}} + \mathbf{B}\dot{\mathbf{E}} + \mathbf{K}\mathbf{E} = (1 - p(t))\,\mathbf{F}_E(t). \tag{25}$$

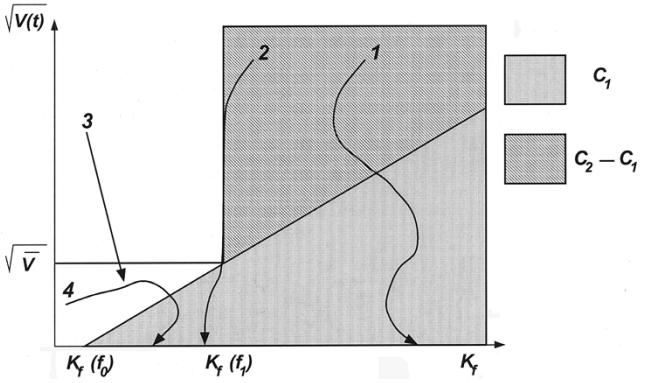

Fig. 2. $\sqrt{V(t)}$ versus $\kappa_f(t) = (1/2)^E M_f {}^E\dot{x}_f^2$, where $V(t)$ is the Lyapunov function in (27), $\kappa_f(t)$ is the flywheel energy, and $\bar{V}$ is the ultimate bound in (29). Four sample paths of $(\kappa_f(t), \sqrt{V(t)})$ are shown. In Paths 1 and 2, $V(t) \to 0$, and in Path 3, $V(t)$ becomes ultimately bounded by $\bar{V}$. In Path 4, $V(t) \to 0$ but it is not guaranteed.

Clearly, if $p(t) = 1$ at all times, $(\mathbf{E}, \dot{\mathbf{E}}) \to (\mathbf{0}, \mathbf{0})$ exponentially. Therefore, the remaining issue is to define a nearly invariant region $\mathcal{C}$ so that if the state enters this region, the feedforward cancellation will be permanently turned on without depleting the flywheel energy.

B. Nearly Invariant Region $\mathcal{C}$

We now analyze the shape system control presented above, and determine the nearly invariant region $\mathcal{C}$ in (24). The desired property of $\mathcal{C}$ is that once the state $({}^E\dot{x}_f, \mathbf{E}, \dot{\mathbf{E}})$ enters into $\mathcal{C}$, it remains in its closure. This implies that the feedforward function remains turned on and the energy in the flywheel will not fall below the desired threshold. Readers who wish to skip the derivation can go directly to (30) and (34), where the definition of $\mathcal{C}$ is given.

Proposition 2: The shape system (10) under the control law (19)–(24) has the following properties.

- If the mismatched human/work environment force $\mathbf{F}_E(\cdot)$ is bounded, then $\mathbf{E}(t)$ and $\dot{\mathbf{E}}(t)$ are ultimately bounded.
- If the feedforward action is turned off (i.e., $p(t) = 0$), then the energy in the fictitious flywheel given by $(1/2)^E M_f {}^E\dot{x}_f^2(t)$ is nondecreasing.

Proof: The closed-loop shape system dynamics are given by (25). Since $\mathbf{K}$ and $\mathbf{B}$ are strictly positive definite, it is a linear exponentially stable system driven by $(1 - p(t))\mathbf{F}_E$. Hence, when $\mathbf{F}_E(\cdot)$ is bounded, $\mathbf{E}(t)$ and $\dot{\mathbf{E}}(t)$ are ultimately bounded.

Differentiating the kinetic energy of the flywheel, and using the control law (21), we have

$$\frac{d}{dt}\left[\frac{1}{2}{}^E M_f {}^E\dot{x}_f^2\right] = {}^E T_f {}^E\dot{x}_f = {}^E\dot{x}_f(t)g(t)\dot{\mathbf{E}}^T\mathbf{B}\dot{\mathbf{E}} \geq 0 \tag{26}$$

when $p(t) = 0$. Hence, the kinetic energy of the flywheel does not decrease when the feedforward action is turned off. ■

Remark 1: Notice from (26) in the proof of *Proposition 2* that when $p(t) = 0$, ${}^E\dot{x}_f$ converges implies $\dot{\mathbf{E}} \to \mathbf{0}$, since ${}^E\dot{x}_f \cdot g(t) > 0$.

Remark 2: The ultimate bound in *Proposition 2*, when $p(t) = 0$, can be estimated by a Lyapunov function. The closed-loop shape system (25) represents an exponentially

stable system with $\mathbf{F}_E(t)$ as input. Thus, we can define positive definite matrices $\mathbf{P} \in \Re^{2n\times 2n}$ and $\mathbf{Q} \in \Re^{2n\times 2n}$, and a Lyapunov function

$$V(t) = \frac{1}{2}(\mathbf{E}^T\ \dot{\mathbf{E}}^T)\mathbf{P}\begin{pmatrix}\mathbf{E}\\ \dot{\mathbf{E}}\end{pmatrix} \tag{27}$$

so that, for some $\gamma > 0$ and $\lambda > 0$

$$\begin{aligned}\dot{V}(t) &= -(\mathbf{E}^T\ \dot{\mathbf{E}}^T)\mathbf{Q}\begin{pmatrix}\mathbf{E}\\ \dot{\mathbf{E}}\end{pmatrix} + (\mathbf{E}^T\ \dot{\mathbf{E}}^T)\mathbf{P}\begin{pmatrix}\mathbf{0}\\ \mathbf{M}_E^{-1}\end{pmatrix}\mathbf{F}_E \\ &\le -\gamma\, V(t) + \lambda V^{\frac{1}{2}}(t)\,\|\mathbf{F}_E(t)\|\end{aligned} \tag{28}$$

where γ is the exponential convergence rate (which may be estimated from $\gamma \ge ((\underline{\sigma}[\mathbf{Q}])/(\bar{\sigma}[\mathbf{P}])) > 0$, where $\underline{\sigma}[\cdot]$ and $\bar{\sigma}[\cdot]$ denote the minimum and maximum singular values of their arguments, respectively). Let $F_{\max}$ be the upper bound of $\mathbf{F}_E(\cdot)$ so that $\|\mathbf{F}_E(t)\| \le F_{\max}$, $\forall t$. From (28), the ultimate bound for the Lyapunov function is found to be

$$\bar{V} = \left[\frac{\lambda}{\gamma}F_{\max}\right]^2. \tag{29}$$

Therefore, if $V^{1/2}(0) \le (\lambda/\gamma)F_{\max}$, then $V^{1/2}(t) \le (\lambda/\gamma)F_{\max}$ for all $t \ge 0$. Otherwise, for any $V^{1/2}(0)$, and for any $\epsilon > 0$, there exists $T > 0$, so that $V^{1/2}(t) \le (\lambda/\gamma)F_{\max}+\epsilon$ whenever $t \ge T$.

The ultimate bound in (29) represents the guaranteed coordination performance under kinematic feedback only. However, satisfactory coordination cannot be guaranteed solely by kinematic feedback, since the ultimate bounds are often unreasonably large in practical cases with feasible gain settings (often limited by sampling rates). This highlights the importance of feedforward cancellation to achieve good coordination performance.

Subregion $\mathcal{C}_1$: Let us define a subregion $\mathcal{C}_1 \subset \mathcal{C} \subset \Re^{2n+1}$ in Fig. 2 as

$$\mathcal{C}_1 := \left\{({}^E\dot{x}_f, \mathbf{E}, \dot{\mathbf{E}})|V^{\frac{1}{2}} < \frac{\gamma\delta^E M_f}{4F_{\max}}\left[{}^E\dot{x}_f{}^2 - {f_0}^2\right]\right\} \tag{30}$$

where V is the Lyapunov function in (27), $f_0 > 0$ is the threshold in (22), δ is a positive scalar (given below), and $F_{\max}$ is the bound on $\|\mathbf{F}_E(\cdot)\|$.

Proposition 3 (Invariance of $\mathcal{C}_1$): Suppose that $\mathcal{C}$ in (24) contains $\mathcal{C}_1$ and that $\|\mathbf{F}_E(t \ge t_1)\| < F_{\max}$. If $({}^E\dot{x}_f, \mathbf{E}, \dot{\mathbf{E}}) \in \mathcal{C}_1$ at $t = t_1$, then, for the shape system (10), under the control law (19)–(24), $({}^E\dot{x}_f, \mathbf{E}, \dot{\mathbf{E}}) \in \mathcal{C}_1\ \forall t \ge t_1$.

Proof: Since $\mathcal{C}_1 \subset \mathcal{C}$,$({}^E\dot{x}_f, \mathbf{E}, \dot{\mathbf{E}}) \in \mathcal{C}_1$ at time t implies that $p(t) = 1$. Therefore, from (25), the shape system dynamics are given by

$$\mathbf{M}_E\ddot{\mathbf{E}} + \mathbf{B}\dot{\mathbf{E}} + \mathbf{K}\mathbf{E} = \mathbf{0}.$$

Using the Lyapunov function (27) in *Remark 2*, there are $\delta > 0$ and $\gamma > 0$ so that

$$\begin{aligned}V(t) &= \frac{1}{2}(\mathbf{E}^T\ \dot{\mathbf{E}}^T)\mathbf{P}\begin{pmatrix}\mathbf{E}\\ \dot{\mathbf{E}}\end{pmatrix} \ge \delta^2\|\dot{\mathbf{E}}\|^2 \\ \dot{V}(t) &= -(\mathbf{E}^T\ \dot{\mathbf{E}}^T)\mathbf{Q}\begin{pmatrix}\mathbf{E}\\ \dot{\mathbf{E}}\end{pmatrix} \le -\gamma V(t).\end{aligned}$$

Consider now the energy stored in the flywheel. We have

$$\begin{aligned}\frac{d}{dt}\left(\frac{1}{2}{}^E M_f {}^E\dot{x}_f{}^2\right) &= {}^E T_f {}^E\dot{x}_f = {}^E\dot{x}_f \mathbf{U}_{fb}^T\dot{\mathbf{E}} + {}^E\dot{x}_f\mathbf{U}_{ff}^T\dot{\mathbf{E}} \\ &= {}^E\dot{x}_f g(t)\dot{\mathbf{E}}^T\mathbf{B}\dot{\mathbf{E}} + {\mathbf{F}_E}^T\dot{\mathbf{E}} \\ &\ge -\|\mathbf{F}_E\|\|\dot{\mathbf{E}}\| \ge -\frac{F_{\max}}{\delta}V^{\frac{1}{2}}(t).\end{aligned}$$

Because $\mathcal{C}_1$ is an open set, this inequality can be integrated to at least up to some $t > t_1$ without the state leaving $\mathcal{C}_1$. Using the fact that $V(t) \le e^{-\gamma(t-t_1)}V(t_1)$ on the integral, we have $\forall t \ge t_1$

$$V^{\frac{1}{2}}(t) - V^{\frac{1}{2}}(t_1) \le \frac{\gamma\,\delta\,{}^E M_f}{4F_{\max}}\left[{}^E\dot{x}_f(t)^2 - {}^E\dot{x}_f(t_1)^2\right]. \tag{31}$$

On the other hand, since $({}^E\dot{x}_f, \mathbf{E}, \dot{\mathbf{E}}) \in \mathcal{C}_1$ at $t = t_1$ as defined in (30)

$$V^{\frac{1}{2}}(t_1) - \frac{\gamma\delta^E M_f}{4F_{\max}}{}^E\dot{x}_f{}^2(t_1) < -\frac{\gamma\,\delta\,{}^E M_f}{4F_{\max}}{f_0}^2. \tag{32}$$

Comparing (31) and (32)

$$V^{\frac{1}{2}}(t) < \frac{\gamma\,\delta}{2F_{\max}}\frac{1}{2}{}^E M_f\left[{}^E\dot{x}_f(t)^2 - f_0^2\right]$$

which says that $({}^E\dot{x}_f, \mathbf{E}, \dot{\mathbf{E}}) \in \mathcal{C}_1$ at time t. Since t can be arbitrary, $\mathcal{C}_1$ is invariant. ■

Intersection With the Ultimate Bound: Define f_1 to be the threshold for the flywheel energy, s.t.

$$\frac{\gamma\delta^E M_f}{4F_{\max}}\left[{f_1}^2 - {f_0}^2\right] = \bar{V}^{\frac{1}{2}} + \epsilon = \frac{\lambda}{\gamma}F_{max} + \epsilon \tag{33}$$

where $\epsilon > 0$ is a small number. The rationale for the definition of f_1 is that the boundary of $\mathcal{C}_1$ intersects with the ultimate bound in *Remark 2* when $\|{}^E\dot{x}_f\| = f_1$. The regions $\mathcal{C}$, $\mathcal{C}_1$, and the relationships with the threshold f_1, and the ultimate bound $\bar{V}$ are illustrated in Fig. 2.

Nearly Invariant Region $\mathcal{C}$: We are now ready to define the *region* $\mathcal{C}$ to be

$$\mathcal{C} := \mathcal{C}_1 \cup \left\{({}^E\dot{x}_f, \mathbf{E}, \dot{\mathbf{E}})\|{}^E\dot{x}_f| > f_1\right\}. \tag{34}$$

Theorem 1: Consider the shape system (15) under the control law (19)–(24), where $\mathcal{C}$ in (24) is given by (34).

1) The closed-loop shape system is passive in the sense that there exists $c^2 > 0$ such that for all $t \ge 0$ and for any mismatched environment force $\mathbf{F}_E(\cdot)$

$$\int_0^t \mathbf{F}_E^T(\tau)\dot{\mathbf{E}}(\tau)d\tau \ge -c^2.$$

2) Suppose that $\|\mathbf{F}_E(t)\| \le F_{\max}\ \forall t \ge 0$. For any initial condition $({}^E\dot{x}_f(0), \mathbf{E}(0), \dot{\mathbf{E}}(0))$, the Lyapunov function $V(t)$ in (27) will be ultimately bounded by $\bar{V}$ in (29).
3) Suppose again that $\|\mathbf{F}_E(t)\| \le F_{\max}$ for all $t \ge 0$. If the state $({}^E\dot{x}_f, \mathbf{E}, \dot{\mathbf{E}})$ lies in the region $\mathcal{C}$ defined in (34) at time t_1, then for all $t \ge t_1$, it will remain in $\overline{\mathcal{C}}$, the closure of $\mathcal{C}$.

4) Furthermore, if $({}^{E}\dot{x}_f(0), \mathbf{E}(0), \dot{\mathbf{E}}(0)) \in \mathcal{C}$, then $\mathbf{E}(t) \to \mathbf{0}$, $\dot{\mathbf{E}}(t) \to \mathbf{0}$, and $|{}^{E}\dot{x}_f(t)| \geq f_0 \forall t \geq 0$.
5) If ${}^{E}\dot{x}_f(0) \neq 0$ and $(\mathbf{E}, \dot{\mathbf{E}}) \not\to 0$, then $\dot{\mathbf{E}}(t) \to \mathbf{0}$.

Proof:

1) Passivity has already been demonstrated for the controller structure of the form (19).
2) This is just a restatement of *Proposition 2* and *Remark 2*.
3) *Proposition 3* shows that the subregion $\mathcal{C}_1$ is invariant. If the initial state belongs to $\mathcal{C}$ but does not belong to $\mathcal{C}_1$, then:
   1) $|{}^{E}\dot{x}_f(t)| \geq f_1$ until the state enters $\mathcal{C}_1$;
   2) eventually, $V(t) \leq \bar{V} + \epsilon$ where ϵ is defined in (33).

   The first result is due to the fact that $|{}^{E}\dot{x}_f(t_1)| > f_1$ and that if ever $|{}^{E}\dot{x}_f(t)| = f_1$ at some time t, feedforward action is turned off, and by *Proposition 2*, the flywheel energy is nondecreasing. Thus, as illustrated in Fig. 2, the state will not cross to the left of the $\kappa_f(f_1)$ line. The second result is due to the ultimate boundedness result (*Remark 2*) so that the state must enter the ultimate bound while maintaining $|{}^{E}\dot{x}_f(t)| \geq f_1$ before entering $\mathcal{C}_1$. Because of the way that f_1 is defined, the state must eventually enter $\mathcal{C}_1$ and remain there (see Fig. 2).
4) Since the state enters $\mathcal{C}_1$ eventually, the feedforward action will be permanently turned on and $(\mathbf{E}(t), \dot{\mathbf{E}}(t)) \to \mathbf{0}$ exponentially from then onwards.
5) If $(\mathbf{E}, \dot{\mathbf{E}}) \not\to 0$, then the state does not enter $\mathcal{C}$. From *Proposition 2*, this means that $V(t)$ would be ultimately bounded, and the energy in the flywheel would be nondecreasing and $|{}^{E}\dot{x}_f(t)| \geq |{}^{E}\dot{x}_f(0)| \geq 0$ for all $t \geq 0$. Since the state does not enter $\mathcal{C}$, $|{}^{E}\dot{x}_f| \leq f_1$. Being an upper bounded, nondecreasing signal, $|{}^{E}\dot{x}_f(t)|$ must converge. From *Remark 1* following *Proposition 2*, this implies that $\dot{\mathbf{E}} \to \mathbf{0}$. ■

Roughly speaking, the shape system control presented above consists of a spring/damper term for stabilization, and the feedforward action to cancel out the effect of $\mathbf{F}_E$ so as to achieve rigid coordination. The innovation of the controller lies in the fact that it makes use of the energy stored in the fictitious flywheel to ensure that the closed-loop system is energetically passive with the feedforward control. As such, passivity is ensured by the controller structure, and does not depend on the accuracy of the force measurement. Also, when the flywheel energy is appropriately initialized (so the initial state lies in $\mathcal{C}$), perfect coordination can be achieved for mismatched human/work environment forces $\mathbf{F}_E$ of arbitrary bandwidth.

In *Theorem 1*, we can only show that $(\mathbf{E}, \dot{\mathbf{E}}) \to (\mathbf{0}, \mathbf{0})$ if the system state enters the region $\mathcal{C}$. Otherwise, $\mathbf{E}$ would only be ultimately bounded. In reality, however, the state is likely to eventually enter $\mathcal{C}$ or $(\mathbf{E}, \dot{\mathbf{E}}) \to (\mathbf{0}, \mathbf{0})$ if the shape system is constantly being excited by time varying mismatched environment/human force $\mathbf{F}_E(t)$. The reason is that if $\mathbf{F}_E(t)$ excites the system (25) perpetually, it is not likely that $\dot{\mathbf{E}}(t) \to \mathbf{0}$, which by *Theorem 1*, Item 5, is a necessity for $\mathbf{E}(t) \not\to \mathbf{0}$. Thus, an operator can shake up the teleoperator first in order to cause the state to enter $\mathcal{C}$ before using the teleoperator for manipulation. Hereafter, if the measurement of $\mathbf{F}_E$ is accurate, then $\mathcal{C}$ will be invariant, and the teleoperator will become rigidly coordinated.

V. Locked System Control

We now consider the control that installs some desirable, target dynamics for the common rigid mechanical tool that the teleoperator aims to mimic.

A. Target Locked System

The *target locked system dynamics* specify the desired dynamics of the common rigid mechanical tool and how it interacts with the human and work environment forces. Expressed in the units and dimension of the master robot (robot 1), they are given by

$$\beta \mathbf{M}_L \ddot{\mathbf{q}}_L + \mathbf{C}_L(\mathbf{q}_L, \dot{\mathbf{q}}_L)\dot{\mathbf{q}}_L = \rho \alpha^{-T}\mathbf{F}_1 + \mathbf{F}_2 = \mathbf{F}_L \quad (35)$$

where $\rho > 0$ is the desired power scaling, $\beta > 0$ is the apparent inertia scaling factor, and $\mathbf{M}_L$ is the unscaled ($\beta = 1$) apparent inertia of the teleoperator in (9). Since the apparent inertia has effects on transparency and how the operator uses the system, the ability to adjust β is useful. The $n \times n$ skew-symmetric matrix

$$\mathbf{C}_L(\mathbf{q}_L, \gamma\dot{\mathbf{q}}_L) = -\mathbf{C}_L(\mathbf{q}_L, \gamma\dot{\mathbf{q}}_L)^T = \gamma \mathbf{C}_L(\mathbf{q}_L, \dot{\mathbf{q}}_L)$$

specifies the unforced natural dynamics of the system. This defines formally an affine connection [31]. It can be designed to facilitate the accomplishment of tasks, and for path guidance or obstacle avoidance.

The target system (35) can also be "pulled back" to be expressed in the units and dimensions of the slave robot (robot 2). In this case

$$\beta \mathbf{M}'_L \ddot{\mathbf{q}}'_L + \mathbf{C}'_L(\mathbf{q}'_L, \dot{\mathbf{q}}'_L)\dot{\mathbf{q}}'_L = \mathbf{F}_1 + \frac{1}{\rho}\alpha^T \mathbf{F}_2 \quad (36)$$

where $\mathbf{q}'_L = \alpha^{-1}\mathbf{q}_L$, $\mathbf{M}'_L = \mathbf{M}_1 + (1/\rho)\alpha^T \mathbf{M}_2 \alpha$, and $\mathbf{C}'_L(\mathbf{q}'_L, \mathbf{q}'_L) = (1/\rho)\alpha^T \mathbf{C}_L(\alpha\mathbf{q}'_L, \alpha\dot{\mathbf{q}}'_L)\alpha$.

Our goal is that when $\mathbf{q}_L$ is identified by

$$\mathbf{q}_L = \frac{\zeta}{\zeta + \rho}\left[\frac{\rho}{\zeta}\alpha\mathbf{q}_1 + \mathbf{q}_2\right] \quad (37)$$

then the target dynamics (35) is achieved. Note that $\dot{\mathbf{q}}_L = \mathbf{V}_L$. Moreover, if $(\mathbf{E}, \dot{\mathbf{E}}) = (0, 0)$, $\mathbf{q}_L = \mathbf{q}_2 = \alpha\mathbf{q}_1$.

B. Locked System Control Law

A control law that would achieve the target locked system dynamics is

$$\mathbf{T}_L = -\frac{1}{\beta}\mathbf{C}_L(\mathbf{q}_L, \mathbf{V}_L)\mathbf{V}_L - \frac{\beta - 1}{\beta}\mathbf{F}_L. \quad (38)$$

Similar to the shape system control, when $\beta \neq 1$, direct implementation of (38) does not robustly preserve passivity of the closed-loop system.

To remedy this problem, we augment the locked system with dynamics of a fictitious flywheel for temporary energy storage, as in the case of the shape system control

$$\begin{bmatrix} \mathbf{M}_L & \mathbf{0} \\ \mathbf{0} & {}^{L}M_f \end{bmatrix} \begin{pmatrix} \dot{\mathbf{V}}_L \\ {}^{L}\ddot{x}_f \end{pmatrix} = \begin{pmatrix} \mathbf{T}_L + \mathbf{F}_L \\ {}^{L}T_f \end{pmatrix} \quad (39)$$

where ${}^{L}M_f > 0 \in \Re$ and ${}^{L}x_f \in \Re$ are the inertia and the configuration of the flywheel, respectively. Define the total energy of the *augmented locked system* by

$$\kappa_L(t) = \frac{1}{2}\mathbf{V}_L^T\mathbf{M}_L\mathbf{V}_L + \frac{1}{2}{}^{L}M_f{}^{L}\dot{x}_f{}^{2}. \tag{40}$$

Consider the following locked system control law:

$$\begin{pmatrix}\mathbf{T}_L\\ {}^{L}T_f\end{pmatrix} = \underbrace{\begin{bmatrix}-(1+\mu)\mathbf{C}_L(\mathbf{q}_L,\mathbf{V}_L) & \mu g_L(t)\mathbf{F}_L\\ -\mu g_L(t)\mathbf{F}_L{}^{T} & 0\end{bmatrix}}_{\mathbf{\Omega}_L(t)}\begin{pmatrix}\mathbf{V}_L\\ {}^{L}\dot{x}_f\end{pmatrix} \tag{41}$$

where $\mu := ((1-\beta)/\beta) > -1$ and

$$g_L(t) := \begin{cases}\frac{1}{{}^{L}\dot{x}_f(t)} & |{}^{L}\dot{x}_f(t)| > {}^{L}f_0\\ \frac{1}{{}^{L}f_0}\text{sign}\left({}^{L}\dot{x}_f(t)\right) & 0 < |{}^{L}\dot{x}_f(t)| \le {}^{L}f_0\\ \frac{1}{{}^{L}f_0} & |\dot{x}_f(t)| = 0\end{cases} \tag{42}$$

is a threshold function to ensure the matrix $\mathbf{\Omega}_L(t)$ does not become unbounded.

Clearly, $\mathbf{T}_L$ in (41) will be exactly (38) when the flywheel speed is above threshold ($|{}^{L}\dot{x}_f(t)| \ge f_0$), since flywheel energy is used to generate the control action to scale up/down the apparent inertia. Notice, however, when no inertia scaling is needed ($\beta = 1$), the flywheel augmentation in (41) is not necessary to preserve passivity.

Theorem 2: The augmented locked system (39) with the control law (41), (42) has the following properties.

1) The closed-loop locked system is passive in the sense of (14) regardless of the accuracy of the force sensor measurements $\mathbf{F}_L$.
2) Suppose that the operating speed $\mathbf{V}_L(\cdot)$ is bounded and the flywheel speed ${}^{L}\dot{x}_f$ has been initialized so that

$$\frac{1}{2}{}^{L}M_f{}^{L}\dot{x}_f{}^{2}(0) > \frac{1}{2}{}^{L}M_f{f_0}^2 + |1-\beta|\bar{E}_L \tag{43}$$

where f_0 is the threshold in (22), and $\bar{E}_L > 0$ is the upper bound that satisfies $(1/2)\mathbf{V}_L(t)^T\mathbf{M}_L\mathbf{V}_L(t) < \bar{E}_L\ \forall t \ge 0$. Then, the *target locked system dynamics* (35) is achieved when the locked system coordinate $\mathbf{q}_L$ is defined as in (37).

Proof:

1) Differentiating the augmented locked system energy function $\kappa_L(\mathbf{V}_L, {}^{L}\dot{x}_f)$ in (40), and using the fact that $\mathbf{\Omega}_L(t)$ in (40) is skew symmetric, we have

$$\frac{d}{dt}\kappa_L(\mathbf{V}_L, {}^{L}\dot{x}_f) = \mathbf{F}_L^T\mathbf{V}_L. \tag{44}$$

The passivity property in (14) is obtained on integration. Since the measurement of $\mathbf{F}_L$ is only used in $\mathbf{\Omega}_L(t)$ which is skew symmetric regardless, passivity does not depend on the measurement accuracy of $\mathbf{F}_L$.
2) Since (41) generates the ideal locked system control (38) when the flywheel speed is above the threshold, it suffices to show that $|{}^{L}\dot{x}_f(t)| \ge f_0$ for all $t \ge 0$.

Using the control law (41), (44), and the definition for $\kappa_L(\cdot,\cdot)$, we have

$$\begin{aligned}&\frac{d}{dt}\left(\frac{1}{2}{}^{L}M_f{}^{L}\dot{x}_f^2\right)\\ &\quad= -\mu\cdot{}^{L}\dot{x}_f g_L(t)\mathbf{F}_L^T\mathbf{V}_L\\ &\quad= -\mu\cdot{}^{L}\dot{x}_f g_L(t)\frac{d}{dt}\left\{\frac{1}{2}{}^{L}M_f{}^{L}\dot{x}_f^2 + \frac{1}{2}\mathbf{V}_L^T\mathbf{M}_L\mathbf{V}_L\right\}\\ &\quad= -\frac{\mu\cdot{}^{L}\dot{x}_f g_L(t)}{1+\mu\cdot{}^{L}\dot{x}_f g_L(t)}\frac{d}{dt}\left\{\frac{1}{2}\mathbf{V}_L^T\mathbf{M}_L\mathbf{V}_L\right\}.\end{aligned} \tag{45}$$

Suppose that ${}^{L}\dot{x}_f{}^{2}(0)$ has been initialized appropriately as in (43). Then, there exists $t > 0$ so that $\forall\,\tau \in [0,t)$, $|{}^{L}\dot{x}_f(\tau)| > f_0$ and $g_L(\tau){}^{L}\dot{x}_f(\tau) = 1$. Integrating (45) with $\mu > -1$, we have

$$\begin{aligned}&\frac{1}{2}{}^{L}M_f\left({}^{L}\dot{x}_f{}^{2}(t) - {}^{L}\dot{x}_f{}^{2}(0)\right)\\ &\quad\ge -\left(\frac{|\mu|}{1+\mu}\right)\frac{1}{2}\left|\mathbf{V}_L^T(t)\mathbf{M}_L\mathbf{V}_L(t) - \mathbf{V}_L^T(0)\mathbf{M}_L\mathbf{V}_L(0)\right|\\ &\quad\ge -\left(\frac{|\mu|}{1+\mu}\right)\bar{E}_L = -|1-\beta|\bar{E}_L.\end{aligned}$$

Given the initialization (43) and from the above, the flywheel energy does not deplete below the threshold f_0 for all $t \ge 0$. ■

VI. Robust Passivity

In Sections IV and V, it has been shown that the shape system control law (19)–(24), where $\mathcal{C}$ in (34), and the locked system control law (41), (42) ensure that the closed-loop shape and locked systems are passive in the sense of (14), even in the presence of inaccurate force measurements. Therefore, by *Proposition 1*, the complete closed-loop system is passive in the sense of (4) and (5). We now show that the proposed control also preserves passivity in the presence of model uncertainty, i.e., when the transformation $\mathbf{S} \in \Re^{2n\times 2n}$ in (7) is inaccurate.

Suppose that $\widehat{\mathbf{S}} \in \Re^{2n\times 2n}$ is an estimate of $\mathbf{S}$ in (7), and let

$$\begin{pmatrix}\widehat{\mathbf{V}}_L\\ \dot{\widehat{\mathbf{E}}}\end{pmatrix} = \widehat{\mathbf{S}}\begin{pmatrix}\dot{\mathbf{q}}_1\\ \dot{\mathbf{q}}_2\end{pmatrix},\quad \begin{pmatrix}\rho\mathbf{T}_1\\ \mathbf{T}_2\end{pmatrix} = \widehat{\mathbf{S}}^T\begin{pmatrix}\widehat{\mathbf{T}}_L\\ \widehat{\mathbf{T}}_E\end{pmatrix} \tag{46}$$

be the estimated locked and shape systems coordinates, and the actual control efforts given to the master and the slave robots. The estimated shape and locked system control, $\widehat{\mathbf{T}}_E$, and $\widehat{\mathbf{T}}_L$ are computed according to (19)–(24), and (41), (42) using $\widehat{\mathbf{V}}_L$ and $\dot{\widehat{\mathbf{E}}}$.

Using the scaled kinetic energy function (6) as the storage function, and from (1), we will have the desired passivity property (4) and (5) if there exists some $d^2 > 0$ such that the control inputs $\mathbf{T}_1(\cdot)$, $\mathbf{T}_2(\cdot)$ satisfies

$$\int_0^t \left[\rho\mathbf{T}_1^T\dot{\mathbf{q}}_1 + \mathbf{T}_2^T\dot{\mathbf{q}}_2\right]d\tau \le d^2 \qquad \forall t \ge 0. \tag{47}$$

The condition in (47) means that the amount of energy generated by the controller is limited. Using (46), (47) is equivalent to

$$\int_0^t \left[\widehat{\mathbf{T}}_L^T\widehat{\mathbf{V}}_L + \widehat{\mathbf{T}}_E^T\dot{\widehat{\mathbf{E}}}\right]d\tau \le d^2. \tag{48}$$

Recall that the shape and locked system controls are of the form

$$\begin{pmatrix} \mathbf{K}\dot{\widehat{\mathbf{E}}} \\ \widehat{\mathbf{T}}_E \\ {}^E M_f {}^E\ddot{x}_f \end{pmatrix} = \mathbf{\Omega}_E(t) \begin{pmatrix} \widehat{\mathbf{E}} \\ \dot{\widehat{\mathbf{E}}} \\ {}^E\dot{x}_f \end{pmatrix} \tag{49}$$

$$\begin{pmatrix} \widehat{\mathbf{T}}_L \\ {}^L M_f {}^L\ddot{x}_f \end{pmatrix} = \mathbf{\Omega}_L(t) \begin{pmatrix} \widehat{\mathbf{V}}_L \\ {}^L\dot{x}_f \end{pmatrix} \tag{50}$$

where $\mathbf{\Omega}_E(t)$ is negative semidefinite, and $\mathbf{\Omega}_L(t)$ is skew symmetric.

Proposition 4: Suppose that the shape system (19)–(24) and the locked system control (41), (42) and the actual control efforts are computed and generated according to (46), where $\widehat{\mathbf{S}} \in \Re^{2n\times 2n}$ is an invertible, but possibly inaccurate estimate of $\mathbf{S}$ in (7). Then the closed–loop dynamics of the teleoperator is passive in the sense of (4) and (5).

Proof: Consider the controller storage function

$$\kappa_c(t) = \frac{1}{2}{}^E M_f {}^E\dot{x}_f{}^2(t) + \frac{1}{2}{}^L M_f {}^L\dot{x}_f^2 + \frac{1}{2}\widehat{\mathbf{E}}^T\mathbf{K}\widehat{\mathbf{E}}.$$

Differentiating $\kappa_c(t)$ and using (49) and (50), we have

$$\begin{aligned} \frac{d}{dt}\kappa_c(t) &= \begin{pmatrix} \widehat{\mathbf{E}}^T & \dot{\widehat{\mathbf{E}}}^T & {}^E\dot{x}_f \end{pmatrix} \mathbf{\Omega}_E(t) \begin{pmatrix} \widehat{\mathbf{E}} \\ \dot{\widehat{\mathbf{E}}} \\ {}^E\dot{x}_f \end{pmatrix} \\ &\quad + \begin{pmatrix} \widehat{\mathbf{V}}_L^T & {}^L\dot{x}_f \end{pmatrix} \mathbf{\Omega}_L(t) \begin{pmatrix} \widehat{\mathbf{V}}_L \\ {}^L\dot{x}_f \end{pmatrix} \\ &\quad - \left[\widehat{\mathbf{T}}_L^T\dot{\widehat{\mathbf{V}}}_L + \widehat{\mathbf{T}}_E^T\dot{\widehat{\mathbf{E}}}\right] \\ &\le - \left[\widehat{\mathbf{T}}_L^T\dot{\widehat{\mathbf{V}}}_L + \widehat{\mathbf{T}}_E^T\dot{\widehat{\mathbf{E}}}\right]. \end{aligned}$$

Integrating this last inequality, and using the fact that $\kappa_c(t) \ge 0$, we obtain (47) with $d^2 = \kappa_c(0)$. ∎

Therefore, the proposed controller structure enforces passivity property of the closed loop even in the presence of inaccurate force measurement and model uncertainty. These nonideal situations affect only performance in terms of coordination or the accuracies in duplicating the target locked system dynamics. In fact, the control law structure will also preserve passivity for *nonlinear* teleoperators, as long as they are open-loop passive in the sense that there exists $c \in \Re$ such that for all t, and $\mathbf{T}_1$, $\mathbf{F}_1$, $\mathbf{T}_2$, $\mathbf{F}_1$

$$\int_0^t \rho(\mathbf{T}_1 + \mathbf{F}_1)\dot{\mathbf{q}}_1 + (\mathbf{T}_2 + \mathbf{F}_2)\,\dot{\mathbf{q}}_2 d\tau \ge -c^2.$$

VII. Application to Nonlinear Teleoperated Manipulators

Although the LDS assumption in Section II can be thought of as an idealization and approximation of a more general class of nonlinear teleoperated manipulators with similar inertia distribution property, strict adherence is very restrictive. In this section, we discuss what happens when the control law designed based on the LDS assumption is actually applied to a multi-DOF *nonlinear* teleoperated manipulator system. Let a pair of n-DOF nonlinear manipulators be of the form

$$\rho\mathbf{M}_1(\mathbf{q}_1)\ddot{\mathbf{q}}_1 + \rho\mathbf{C}_1(\mathbf{q}_1,\dot{\mathbf{q}}_1)\dot{\mathbf{q}}_1 = \rho\mathbf{F}_1 + \rho\mathbf{T}_1 \tag{51}$$

$$\mathbf{M}_2(\mathbf{q}_2)\ddot{\mathbf{q}}_2 + \mathbf{C}_2(\mathbf{q}_2,\dot{\mathbf{q}}_2)\dot{\mathbf{q}}_2 = \mathbf{F}_2 + \mathbf{T}_2 \tag{52}$$

where ρ is the power scaling factor, $\mathbf{M}_1(\mathbf{q}_1)$, $\mathbf{M}_2(\mathbf{q}_1)$ are the upper and lower bounded nonlinear inertia matrices, and $\mathbf{C}_1(\cdot,\cdot)$ and $\mathbf{C}_2(\cdot,\cdot)$ are the associated Coriolis matrices. Without loss of generality, assume that both robots share the same configuration spaces, i.e., $\mathcal{G}_1 := \{\mathbf{q}_1\} = \mathcal{G}_2 := \{\mathbf{q}_2\}$, and the coordination requirement is given by $\mathbf{q}_1 \to \mathbf{q}_2$ (i.e., α is the identity map). In general, if the coordination requirement is given by $\alpha(\mathbf{q}_1) = \mathbf{q}_2$ where $\alpha : \mathcal{G}_1 \to \mathcal{G}_2$ is a smooth invertible map, the above assumption can be achieved if we use $\mathbf{q}_1' = \alpha(\mathbf{q}_1)$ instead of $\mathbf{q}_1$ as the coordinates when deriving (51).

An *approximate* LDS system can be obtained by choosing a positive definite constant matrix $\mathbf{M} \in \Re^{n\times n}$ and a scalar $\zeta > 0$ so that

$$\zeta\mathbf{M} \approx \zeta\mathbf{M}_1(\mathbf{q}_1) \approx \mathbf{M}_2(\mathbf{q}_1) \tag{53}$$

for all $\mathbf{q}_1$ in the operating region of interest. A pair of nonlinear manipulators is said to be dynamically similar after coordination, if $\zeta\mathbf{M}_1(\mathbf{q}_1) = \mathbf{M}_2(\mathbf{q}_1)$ for all $\mathbf{q}_1 \in \Re^n$.

Let $\mathbf{T}_E$ and $\mathbf{T}_L$ be the shape system and the locked system control determined in Sections IV and V, respectively. Notice that they require knowledge of ζ but not $\mathbf{M}$ specifically. They are converted to actual control inputs $\mathbf{T}_1$ and $\mathbf{T}_2$ via (8) with $\alpha = \mathbf{I}$.

Consider first the dynamics of the nonlinear manipulators, supposing that (51) and (52) are rigidly coordinated with $\mathbf{q}_1(t) \equiv \mathbf{q}_2(t)$. Using the transformation (8), and imposing the holonomic constraint $\mathbf{q} = \mathbf{q}_1 = \mathbf{q}_2$, the resulting nonlinear *locked* system dynamics are given by

$$\mathbf{M}_{nL}(\mathbf{q})\ddot{\mathbf{q}} + \mathbf{C}_{nL}(\mathbf{q},\dot{\mathbf{q}})\dot{\mathbf{q}} = \underbrace{(\rho\mathbf{F}_1 + \mathbf{F}_2)}_{\mathbf{F}_L} + \underbrace{(\rho\mathbf{T}_1 + \mathbf{T}_2)}_{\mathbf{T}_L} \tag{54}$$

where

$$\mathbf{M}_{nL}(\mathbf{q}) = \rho\mathbf{M}_1(\mathbf{q}) + \mathbf{M}_2(\mathbf{q})$$
$$\mathbf{C}_{nL}(\mathbf{q},\dot{\mathbf{q}}) = \rho\mathbf{C}_1(\mathbf{q},\dot{\mathbf{q}}) + \mathbf{C}_2(\mathbf{q},\dot{\mathbf{q}})$$

are, in fact, the inertia and the Coriolis matrices if (51) and (52) are under the holonomic constraint $\mathbf{q}_1 \equiv \mathbf{q}_2$.

Notice that (54) does not depend on the shape system control $\mathbf{T}_E$. With the LDS locked system control given by

$$\mathbf{T}_L = -\frac{1}{\beta}\mathbf{C}_L(\mathbf{q},\dot{\mathbf{q}})\dot{\mathbf{q}} - \frac{\beta-1}{\beta}\mathbf{F}_L$$

when the locked system flywheel speed is above the threshold, the resulting dynamics are given by

$$\beta\mathbf{M}_{nL}(\mathbf{q})\ddot{\mathbf{q}} + [\beta\mathbf{C}_{nL}(\mathbf{q},\dot{\mathbf{q}}) + \mathbf{C}_L(\mathbf{q},\dot{\mathbf{q}})]\,\dot{\mathbf{q}} = \rho\mathbf{F}_1 + \mathbf{F}_2. \tag{55}$$

Equation (55) should be interpreted to be the nonlinear target locked system dynamics. Thus, if coordination can be achieved, the effect of the LDS control law on the nonlinear teleoperated

manipulators is to scale the nonlinear locked system inertia by β and alter the Coriolis matrix. Note that the matrix

$$\frac{d}{dt}\beta\mathbf{M}_{nL}(\mathbf{q}) - 2\left[\beta\mathbf{C}_{nL}(\mathbf{q},\dot{\mathbf{q}}) + \mathbf{C}_L(\mathbf{q},\dot{\mathbf{q}})\right]$$

which characterizes the passivity property of the closed-loop locked system is skew symmetric.

We now consider the dynamics of the coordination error $\mathbf{E} = (\zeta/(\rho+\zeta))(\mathbf{q}_1 - \mathbf{q}_2)$ and investigate whether $(\mathbf{E}, \dot{\mathbf{E}})$ can indeed be made small as assumed in the locked system analysis above. The LDS shape system controller in Section IV virtually couples the two robots (51) and (52) via a set of constant spring and damper, and imperfectly cancels the effect of external forces $\mathbf{F}_1$ and $\mathbf{F}_2$. The shape system dynamics are given by

$$\mathbf{M}_1(\mathbf{q}_1)\ddot{\mathbf{E}} + \frac{\nu^2}{\rho}\left(\mathbf{I}+\rho\mathbf{M}_1(\mathbf{q}_1)\mathbf{M}_2^{-1}(\mathbf{q}_2)\right)\times(\mathbf{B}\dot{\mathbf{E}}+\mathbf{K}\mathbf{E}) = \mathbf{d}(t) \tag{56}$$

where

$$\begin{aligned}\nu &:= \zeta/(\zeta+\rho) \text{ and}\\ \mathbf{d}(t) &= \frac{\nu^2}{\zeta}(\mathbf{I} - \zeta\mathbf{M}_1\mathbf{M}_2^{-1})(\mathbf{T}_L + \mathbf{F}_L)\\ &\quad - \nu\left[\mathbf{C}_1\dot{\mathbf{q}}_1 - \mathbf{M}_1\mathbf{M}_2^{-1}\mathbf{C}_2\dot{\mathbf{q}}_2\right].\end{aligned}$$

Using the Lyapunov function

$$V = \frac{1}{2\nu^2}\dot{\mathbf{E}}^T\mathbf{M}_V(t)\dot{\mathbf{E}} + \frac{\epsilon}{\nu^2}\dot{\mathbf{E}}^T\mathbf{M}_V(t)\mathbf{E} + \frac{1}{2\rho}\mathbf{E}^T(\epsilon\mathbf{B}+\mathbf{K})\mathbf{E} \tag{57}$$

where $\epsilon > 0$ is a suitably small scalar, and $\mathbf{M}_V(t) = [\mathbf{M}_1^{-1} + \rho\mathbf{M}_2^{-1}]^{-1}$, it can be shown that

$$\begin{aligned}\dot{V} \le &-\dot{\mathbf{E}}^T\left(\frac{1}{\rho}\mathbf{B} - \frac{\epsilon}{\nu^2}\dot{\mathbf{M}}_\upsilon - \frac{1}{2\nu^2}\dot{\mathbf{M}}_\upsilon\right)\dot{\mathbf{E}} - \frac{\epsilon}{\rho}\mathbf{E}^T\mathbf{K}\mathbf{E}\\ &+ \frac{\epsilon}{\nu^2}\dot{\mathbf{E}}^T\dot{\mathbf{M}}_\upsilon\mathbf{E} + (\rho_1\|\mathbf{E}\| + \rho_2\|\dot{\mathbf{E}}\|)\|\mathbf{d}(t)\|\end{aligned}$$

for some $p_1 > 0, p_2 > 0$. Here, p_1, p_2, and the operator norm of $\dot{\mathbf{M}}_\upsilon$ are all bounded when $(\dot{\mathbf{q}}_1, \dot{\mathbf{q}}_2)$ are bounded. Also, $\mathbf{d}(t)$ is bounded when $\mathbf{T}_L, \mathbf{F}_L, \dot{\mathbf{q}}_1, \dot{\mathbf{q}}_2$ are bounded. Furthermore, p_1, p_2, and $\mathbf{d}(t)$ do not depend on $\mathbf{K}$ and $\mathbf{B}$. Therefore, $\mathbf{E}$ and $\dot{\mathbf{E}}$ will be ultimately bounded if $\mathbf{T}_L, \mathbf{F}_L, \dot{\mathbf{q}}_1, \dot{\mathbf{q}}_2$ are bounded. Moreover, the bound can be made arbitrarily small by choosing $\mathbf{K}$ and $\mathbf{B}$ sufficiently large. Alternatively, sliding mode-type robust control as suggested in [18] can be used to eliminate the coordination error. In other words, by using high gain or sliding mode control, the coordination error can be arbitrarily small, so that dynamics of the nonlinear teleoperated manipulator will be close to the nonlinear locked system dynamics (55).

A full analysis of the nonlinear teleoperated manipulators is beyond the scope of this paper and is treated in [28] and [29]. In fact, the somewhat unwieldy Lyapunov function (57) is inspired by the nonlinear analysis in [28].

VIII. Experimental Results

The proposed control law was implemented on the 1-DOF LDS teleoperator system, as well as a pair of 2-DOF nonlinear (non-LDS) teleoperated manipulators, with one robot being simulated on a computer, and the other being an actual robot. This is done partly due to hardware limitations, and partly to demonstrate the suitability of the proposed control law for haptic display and virtual reality applications. The flexibility of computer simulation also allows experimentations with very different inertia properties.

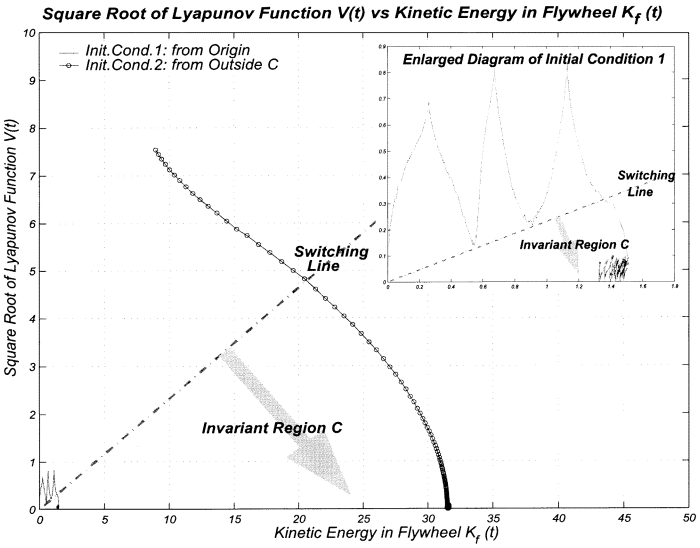

Fig. 3. $\sqrt{V(t)}$-flywheel energy trajectories and the invariant region $\mathcal{C}$ of the two sets of initial conditions. See Fig. 2 for interpretation. The enlarged figure contains the trajectories of the first initial condition. Notice the ripples after entering $\mathcal{C}$ due to noise, actuation ripples, and discretization.

A. 1-DOF LDS Teleoperation Experiments

The 1-DOF LDS system is equipped with a JR^3 force sensor on the master robot, and a custom-built semiconductor-type strain gage force sensor on the slave robot. 50 and 150-Hz low-pass filters are used for the slave and the master force measurements. Control is implemented using MatLab Real-time toolbox at 500-Hz sampling rate. Both kinematic scaling α and power scaling ρ are set to be unity.

Shape and Locked System Control: Consider first the experiment when the inertia scaling is $\beta = 1$, and the human operator manipulates the teleoperator while the slave robot is unconstrained. To illustrate the role that the invariant region $\mathcal{C}$ plays, consider two sets of initial conditions: a) both the shape system flywheel energy and coordination error are initially zero (i.e., starts at the origin in Fig. 3); b) the initial state lies outside of the invariant region $\mathcal{C}$ with nonzero flywheel energy and nonzero coordination error.

The displacement trajectories in both cases are shown in Fig. 4. Fig. 3 shows the trajectories of the Lyapunov function (27) and of the flywheel energy in relation to the invariant region $\mathcal{C}$.

From the first set of initial conditions, the human operator excites the system to generate sufficient energy so that the state of the augmented shape system eventually enters $\mathcal{C}$, and feedforward cancellation is then activated. Before the system enters into $\mathcal{C}$, only kinematic control is used and the coordination performance is poor (error around 5°) due to the mismatched operator/environment force $\mathbf{F}_E$. After the augmented shape system attains enough energy, feedforward cancellation is activated and

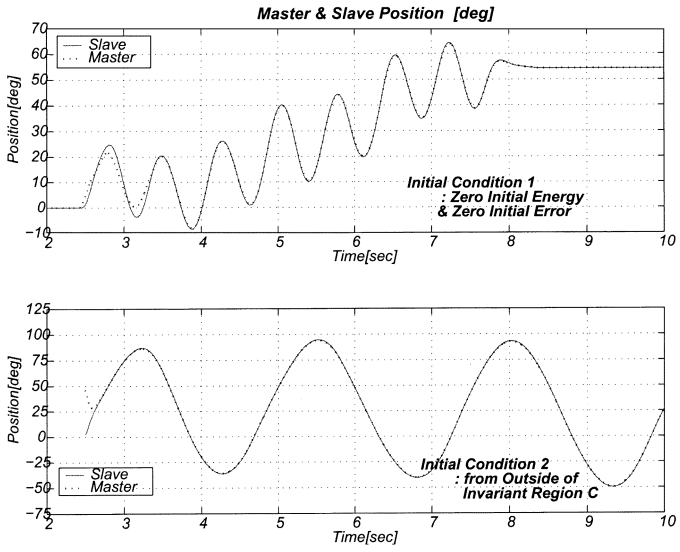

Fig. 4. Position trajectories of the master and the slave manipulators with the two initial conditions. Note that in the first initial condition, the teleoperator achieves locking after the augmented shape system has gained some energy from the human operator.

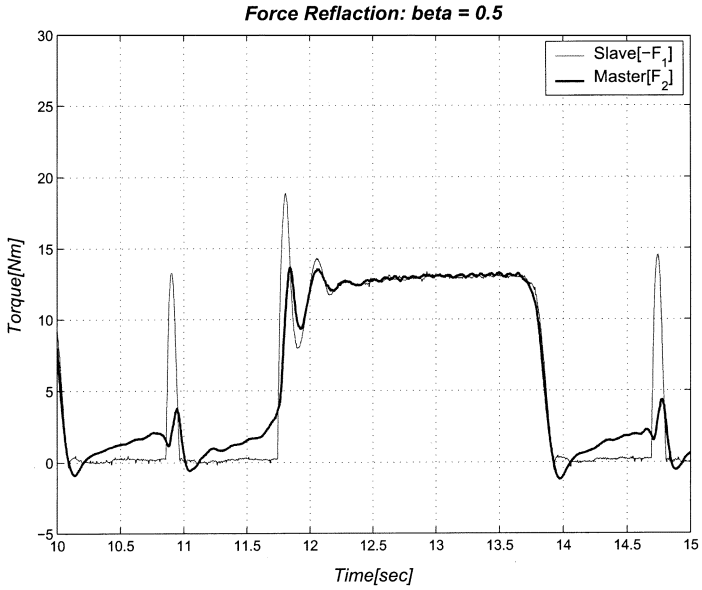

Fig. 5. Master and slave force profiles during hard contact experiment, $\beta = 0.5$.

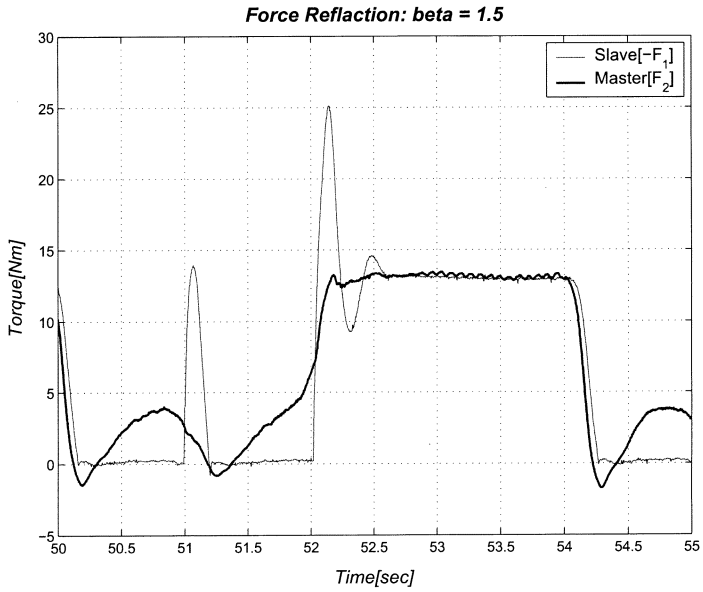

Fig. 6. Master and slave force profiles during hard contact experiment, $\beta = 1.5$.

the coordination error decreases significantly (error less than $0.5°$).

From the second set of initial conditions, both the flywheel energy and the coordination error are set to be nonzero initially. The system starts outside region $\mathcal{C}$, as pointed out in Section IV, the shape system flywheel energy increases when the feedforward is turned off (unless $\dot{\mathbf{E}} = 0$). This causes the state to enter the invariant region $\mathcal{C}$ quickly (after 0.2 s) and the locked system becomes nearly rigidly coordinated thereafter.

The trajectory that results from the first case exhibits some small ripples inside of the invariant region $\mathcal{C}$ (see inset of Fig. 3). We suspect that these are due to measurement noise, actuation ripples, and discretization.

The ultimate bound for the Lyapunov function as predicted by *Remark 2* is too large ($\sqrt{\overline{V}} > 10^4$) to be shown in Fig. 3. This highlights the practical limitation of using kinematic feedback alone, and the necessity for feedforward cancellation to achieve good coordination performance.

Similar tracking errors of less than $0.6°$ are also obtained with the inertia scalings being $\beta = 0.5$ or $\beta = 1.5$ (not shown). It is interesting to note (not shown in plots) that when the apparent inertia is decreased ($\beta < 1$), the unmeasured friction causes the locked system flywheel energy to decrease, and when the apparent inertia is increased ($\beta > 1$), the flywheel energy increases. For this reason, the locked system flywheel speed may need to be saturated or reset occasionally.

Hard Contact and Inertia Scaling: In this experiment, the subject is asked to teleoperate the slave robot to hit an aluminum wall, first with a short impact force and then with a steady force level. The timing is determined by the rhythm of a background music. The target impact and steady force levels are 13–14 Nm. The slave force trajectories are displayed to the subject during the experiment. This simulates a task typical of piano playing (a staccato note followed by a tenuto note). The subject repeats this experiment 40 times. Inertia scalings of $\beta = 0.5$ and $\beta = 1.5$ are used. Control gains are tuned so that the coordination performances are similar for all β's so as to eliminate the differences due to different coordination performance and to focus on inertia scaling only.

Figs. 5 and 6 show the sample force profiles for the apparent inertias of $\beta = 0.5$ and $\beta = 1.5$. Notice for small apparent inertia ($\beta = 0.5$), the master and slave force profiles have similar shapes, compared to $\beta = 1.5$. This indicates a more transparent system with a smaller intervening inertia.

B. Two-DOF Non-LDS Nonlinear Teleoperators

In order to validate the applicability of the proposed control to multi-DOF nonlinear systems, the proposed control is applied to a pair of planar 2-DOF nonlinear manipulators. The

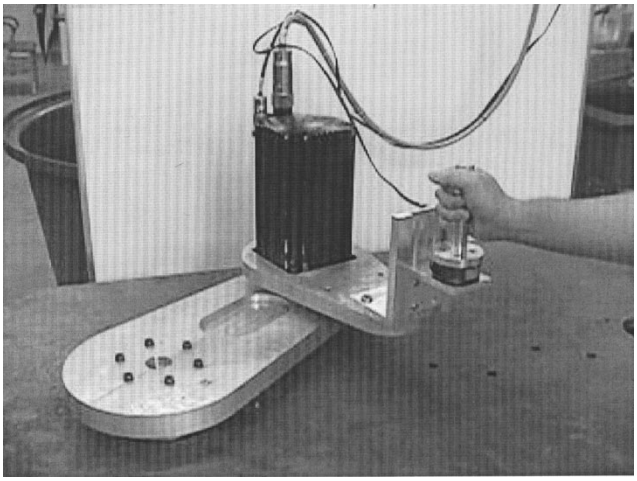

Fig. 7. A 2-DOF planar master robot equipped with a force sensor. The 2-DOF slave robot is implemented as a virtual environment which is simulated in real time.

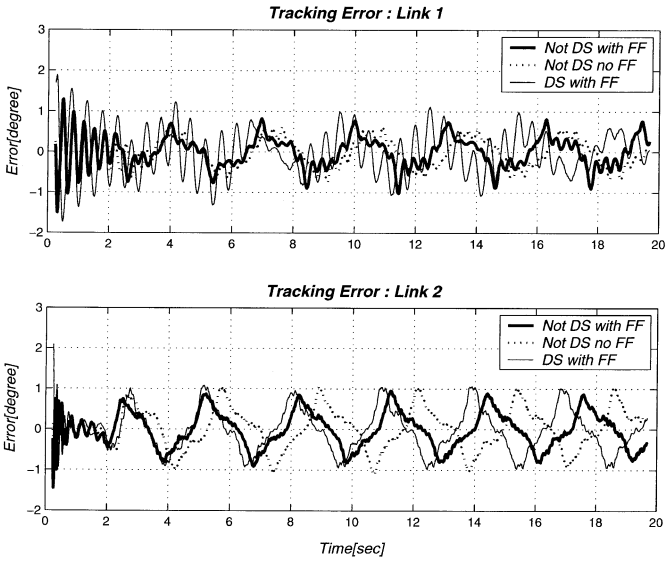

Fig. 8. Coordination error for the tracking experiment with nonlinear teleoperator consisting of two 2-DOF robotic systems for the three cases discussed in the text.

master (Fig. 7) is equipped with a JR^3 force sensor with 120 Hz low-pass filter. The slave robot is a real-time computer simulated virtual environment. The MatLab xPC Target system is used to implement the controller and the virtual environment using a 2 kHz sampling rate.

Three cases are considered:

1) the slave robot has different inertia structure from that of the master (not dynamically similar) with the feedforward cancellation in (16) (Not DS with FF);
2) the slave has the same inertia as case 1) except that the feedforward cancellation in (16) is deactivated (Not DS no FF);
3) and the slave robot inertia structure is identical to the master and the feedforward cancellation is used (DS with FF). The robots are said to be dynamically similar after coordination, but not linear, in this case.

For cases 1) and 2), the inertia matrices of the master and slaves are, respectively, (in Ns^2/m)

$$\mathbf{M}_1(\mathbf{q}) = \begin{bmatrix} 4.06 + 0.38c2 & 0.38 + 0.19c2 \\ 0.38 + 0.19c2 & 0.38 \end{bmatrix} \quad (58)$$

$$\mathbf{M}_2(\mathbf{q}) = \begin{bmatrix} 3.25 + 0.34c2 & 0.57 + 0.17c2 \\ 0.57 + 0.17c2 & 0.57 \end{bmatrix} \quad (59)$$

where $c2$ is cosine of the relative angle between the first and second links. For case 3), $\mathbf{M}_2(\mathbf{q})$ is set to be the same as $\mathbf{M}_1(\mathbf{q})$. Thus, for case 3), $\zeta = 1$. For the other two cases, $\zeta = 1.067$ is used, which minimizes the two-norm error between the two sets of inertia parameters, $[4.06, 0.19, 0.38]$ and $[3.25, 0.17, 0.57]$. Power scaling ($\rho = 2$) and inertia scaling ($\beta = 1/3$) are assumed with kinematic scaling being unity.

Unconstrained Coordination Performance: In case 1), the controller gains are tuned so that coordination errors in both links are less than $\pm 1^\circ$ with typical master position commands. The same gain setting is used in case 2) except that feedforward cancellation is turned off. In case 3), the control gains are detuned and reduced from case 1) to achieve the same level of coordination error as in case 1).

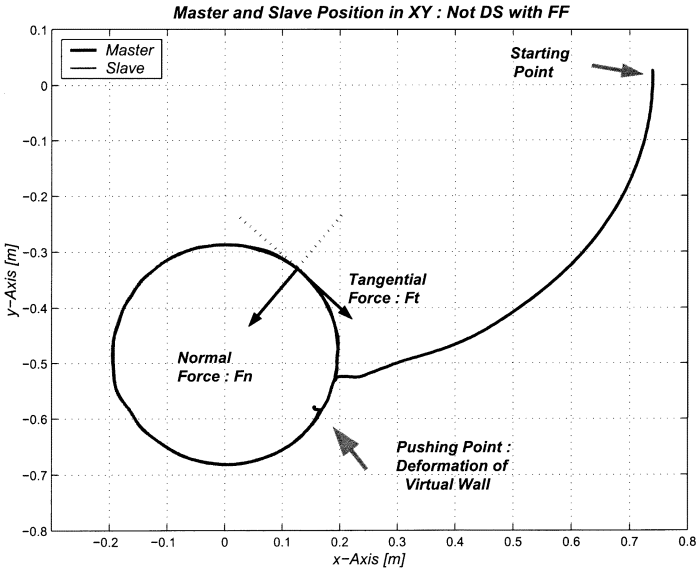

Fig. 9. Motion of the master and slave robots in $x - y$ space with the feedforward cancellation. The slave is a non-dynamically similar system. A circular virtual object is implemented in the slave work environment. A human operator moves the master from the starting point, traces the contour of the virtual object twice, and pushes against the virtual object.

The tracking error for all three cases are shown in Fig. 8. The oscillation during 0–2 s is due to initial position error between the two robots. The steady-state coordination errors in all three cases are very similar. This suggests, at least for small environment forces, that the feedforward control in case 1) is not helpful without a good model, and the coordination performance is achieved by the sufficiently high kinematic gains. Notice that the size of the kinematic gains are limited by sampling rate. When the assumption of dynamical similarity is meaningful, e.g., in case 3) with $\zeta = 1$, feedforward cancellation is effective, since similar level of coordination error is achieved using

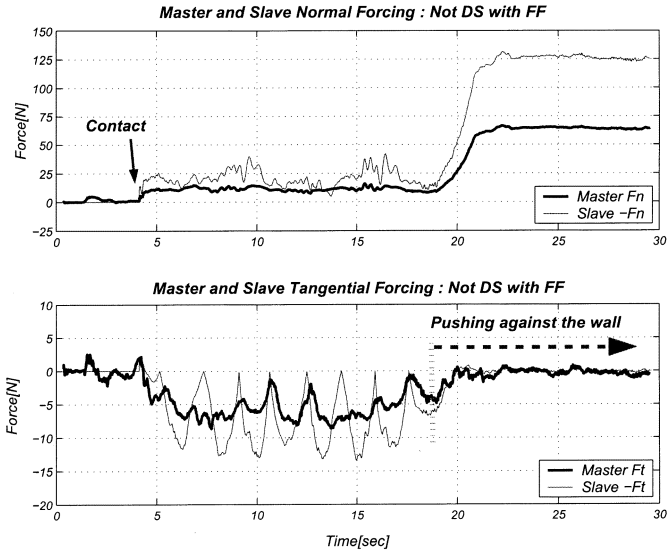

Fig. 10. Force history that the master and slave encounter. For the explanation of normal and tangential force components, please refer to Fig. 9.

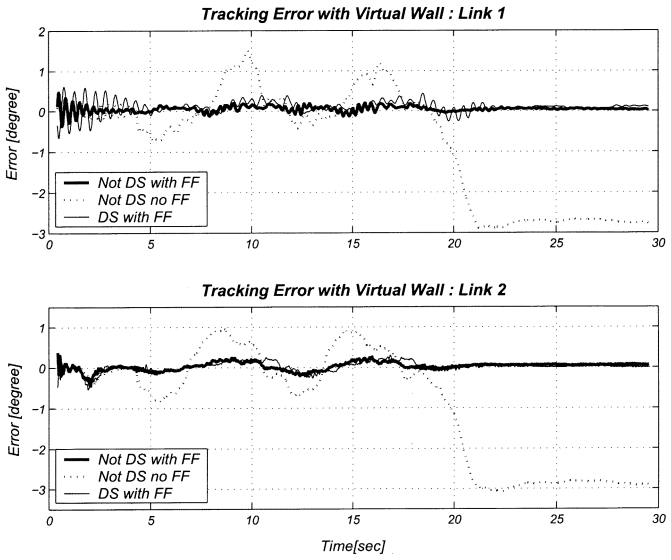

Fig. 11. Coordination error with the virtual object for the three cases. The importance of feedforward cancellation is highlighted by the remarkably worse coordination of case 2) when the human is pushing the teleoperator against the object.

significantly smaller kinematic feedback gain (70% in terms of sum of two eigenvalues of $\mathbf{B}$ and $\mathbf{K}$ in (16)).

Force Reflection Performance: A circular virtual object of radius 20 cm is installed in the workspace of the slave robot (Fig. 9). The stiffness of the object is 7000 N/m to the normal motion and the damping coefficient is 105 Ns/m. Fig. 9 shows the trace of the slave robot end-effector during a maneuver in which the human operator moves toward the object, follows the contour of the object twice, and pushes the robot against the object using as constant a force as he can. Notice the deformation of the virtual object while the operator is pushing against it.

Fig. 10 shows the normal and tangential force histories in the master and the slave robots for case 1) (non-dynamically similar with feedforward control). It shows a force scaling factor of approximately two while the operator is pushing against the object. This is consistent with power scaling $\rho = 2$ when the teleoperator has negligible movement. The tangential force when the operator is moving around the object is generated by damping. The force reflection performances for cases 2) and 3) are similar. So plots are omitted.

Although all three cases have force reflection performances similar to Fig. 10, Fig. 11 shows that during constrained contact, there is a significant degradation in coordination performance when feedforward control is not used [see case 2)], especially when slave contact force is large.

Summary: The proposed control is effective even for non-LDS nonlinear teleoperator. Specifically, feedforward control is useful in reducing the need for high kinematic gains when there is a meaningful dynamical similar (not necessary linear) model for the teleoperator [case 3)]. Moreover, when the environment forces are large (such as in constrained/contact experiments), feedforward control is very important in maintaining good coordination performance between the master and slave robots [case 1) versus case 2)].

IX. Conclusions

In this paper, we have proposed a passive feedforward control scheme for LDS teleoperator systems to achieve both kinematic and power scalings. The control law renders the teleoperator as a common rigid mechanical tool to both the operator and the work environment with an adjustable apparent inertia. Passivity of the closed-loop system is robustly guaranteed, even in the presence of force measurement inaccuracies and model uncertainties. The key ideas of this paper are: 1) a simultaneous dynamic and energetic decomposition of the teleoperator into the shape and the locked systems, which can be controlled separately; 2) a control structure that robustly preserves passivity. Although the proposed control law is derived based on the LDS assumption, it can also be used for general nonlinear teleoperator systems with sufficiently high feedback gains. Furthermore, the passivity of the closed-loop teleoperator is also guaranteed for the nonlinear systems. The control laws have been validated experimentally. Future papers will extend these ideas to nonlinear teleoperators.

References

[1] M. Vidyasagar, *Analysis of Nonlinear Dynamic Systems*, 2nd ed. Englewood Cliffs, NJ: Prentice-Hall, 1993.
[2] N. Hogan, "Controlling impedence at the man/machine interface," in *Proc. IEEE Int. Conf. Robotics and Automation*, 1989, pp. 1626–1631.
[3] R. J. Anderson and M. W. Spong, "Bilateral control of teleoperators with time delay," *IEEE Trans. Automat. Contr.*, vol. 34, pp. 494–501, May 1989.
[4] M. Peshkin and J. E. Colgate, "Cobots," *Ind. Robot*, vol. 26, no. 5, pp. 335–341, 1999.
[5] P. Y. Li and R. Horowitz, "Control of smart exercise machine: Part 1. problem formulation and nonadaptive control," *IEEE/ASME Trans. Mechatron.*, vol. 2, pp. 237–247, Apr. 1997.
[6] B. Hannaford, "A design framework for teleoperators with kinesthetic feedback," *IEEE Trans. Robot. Automat.*, vol. 5, pp. 426–434, Aug. 1989.
[7] Y. Yokokohji and T. Yoshikawa, "Bilateral control of master-slave manipulators for ideal kinesthetic coupling—formulation and experiment," *IEEE Trans. Robot. Automat.*, vol. 10, pp. 605–620, Oct. 1994.
[8] J. E. Colgate, "Robust impedance shaping telemanipulation," *IEEE Trans. Robot. Automat.*, vol. 9, pp. 374–384, Aug. 1993.

[9] D. A. Lawrence, "Stability and transparency in bilateral teleoperation," *IEEE Trans. Robot. Automat.*, vol. 9, pp. 624–637, Oct. 1993.
[10] K. Hashtrudi-Zaad and S. Salcudean, "Adaptive transparent impedence reflecting teleoperation," in *Proc. IEEE Int. Conf. Robotics and Automation*, 1996, pp. 1369–1374.
[11] M. Zhu, W. Zhu, S. Salcudcan, and K. Hashtrudi-Zaad, "Transparent bilateral teleoperation under position and rate control," *Int. J. Robot. Res.*, vol. 19, no. 12, pp. 1185–1202, 2000.
[12] S. Salcudean and N. Wong, "Coarse-fine motion coordination and control of a teleoperation system with magnetically leviated master and wrist," in *Experimental Robotics III*, T. Yoshikawa and F. Miyazaki, Eds. New York: Springer-Verlag, 1993, pp. 28–30.
[13] P. Y. Li, "Passive control of bilateral teleoperated manipulators," in *Proc. American Control Conf.*, 1998, pp. 3838–3842.
[14] J. Doubler and D. Childress, "An analysis of extended physiological proprioception as a prosthesis control technique," *J. Rehab. Res. Devel.*, vol. 21, no. 1, pp. 5–18, 1984.
[15] ——, "Design and evaluation of a prosthesis control system based on the concept of extended physiological proprioception," *J. Rehab. Res. Devel.*, vol. 21, no. 1, pp. 19–31, 1984.
[16] T. Itoh, K. Kosuge, and T. Fukuda, "Human-machine cooperative telemanipulation with motion and force scaling using task-oriented virtual tool dynamics," *IEEE Trans. Robot. Automat.*, vol. 16, pp. 505–516, Oct. 2000.
[17] P. Y. Li and D. Lee, "Passive feedforward approach to bilateral teleoperated manipulators," in *Proc. ASME Dynamic Systems and Control Division*, Orlando, FL, 2000, pp. 1153–1160.
[18] D. Lee and P. Y. Li, "Passive control of bilateral teleoperated manipulators: robust control and experiment," in *Proc. American Control Conf.*, VA, Arlington, 2001, pp. 4612–4618.
[19] T. I. Tsay, H. Kazerooni, and K. Hollerbach, "A controller design framework for telerobotic systems," *IEEE Trans. Contr. Syst. Technol.*, vol. 1, pp. 50–62, Jan. 1993.
[20] H. Kazerooni and C. L. Moore, "An approach to telerobotic manipulations," *ASME J. Dynam. Syst., Meas., Contr.*, vol. 119, no. 3, pp. 431–438, 1997.
[21] N. Wong, S. Salcudean, and R. Hollis, "Design and control of a force-reflecting teleoperation system with magnetically leviated master and wrist," *IEEE Trans. Robot. Automat.*, vol. 11, pp. 844–858, Dec. 1995.
[22] P. Y. Li, "Coordinated contour following control for machining operations—a survey," in *Proc. American Control Conf.*, San Diego, CA, 1999, pp. 4543–4547.
[23] D. Sun and J. K. Mills, "Adaptive synchronized control for coordination of multirobot assembly tasks," *IEEE Trans. Robot. Automat.*, vol. 18, pp. 498–510, Aug. 2002.
[24] P. Y. Li and R. Horowitz, "Passive velocity field control of mechanical manipulators," *IEEE Trans. Robot. Automat.*, vol. 15, pp. 751–763, Aug. 1999.
[25] ——, "Passive velocity field control, part 1: geometry and robustness," *IEEE Trans. Automat. Contr.*, vol. 46, pp. 1346–1359, Sept. 2001.
[26] ——, "Passive velocity field control, part 2: application to contour following problems," *IEEE Trans. Automat. Contr.*, vol. 46, pp. 1360–1371, Sept. 2001.
[27] P. Y. Li, "Adaptive passive velocity field control," in *Proc. American Control Conf.*, 1999, pp. 774–779.
[28] D. Lee and P. Y. Li, "Passive coordination control to nonlinear bilateral teleoperated manipulators," in *Proc. IEEE Int. Conf. Robotics and Automation*, vol. 3, 2002, pp. 3278–3283.
[29] ——, "Passive tool dynamics rendering for nonlinear bilateral teleoperated manipulators," in *Proc. IEEE Int. Conf. Robotics and Automation*, vol. 3, 2002, pp. 3284–3289.
[30] M. Goldfarb, "Similarity and invariance in scaled bilateral telemanipulation," *ASME J. Dynam. Syst., Meas., Contr.*, vol. 121, no. 1, pp. 79–87, 1999.
[31] S. Kobayashi and K. Nomizu, *Foundations of Differential Geometry*. New York: Wiley, 1996, vol. 1.

Dongjun Lee (S'02) received the B.S. degree in mechanical engineering from Korea Advanced Institute of Science and Technology (KAIST), Taejon, Korea, in 1995, and the M.S. degree in automation and design from KAIST, Seoul, Korea, in 1997. He is currently working toward the Ph.D. degree at the University of Minnesota, Twin Cities, Minneapolis-St. Paul.

From 1997 to 1999, he was with Kia Motors Inc., Korea, as an Engine Combustion Development Engineer. His research interests include dynamics and control of mechatronic and robotic systems with emphasis on teleoperation, haptic interface, distributed mechanical systems, and human-interactive robotics.

Mr. Lee is a 2002–2003 Doctoral Dissertation Fellow of the University of Minnesota.

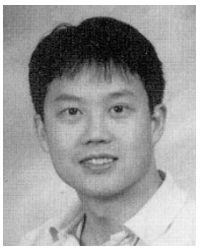

Perry Y. Li (S'87–M'95) received the B.A.(Hons) and M.A. degrees in electrical and information sciences from Cambridge University, Cambridge, U. K. in 1987 and 1990, the M.S. degree in biomedical engineering from Boston University, Boston, MA in 1990, and the Ph.D. degree in mechanical engineering from the University of California, Berkeley in 1995.

He is currently Nelson Assistant Professor in Mechanical Engineering at the University of Minnesota, Twin Cities, Minneapolis-St. Paul. Prior to joining the University of Minnesota in 1997, he was a Researcher at Xerox Corporation, Webster, NY. His research interests are in dynamic systems and control as applied to fluid power systems, robotics, manufacturing, man-machine systems, transportation systems, and imaging and printing.

Dr. Li was awarded the 2000–2002 Japan/USA Symposium on Flexible Automation Young Investigator Award, as well as the Achievement Award and the Special Recognition Awards from Xerox.